ETS-RT - 2016-003

IMPLEMENTATION DETAILS OF A HARDWARE ABSTRACTION-BASED DESIGN METHOLODY FOR RADIOFREQUENCY CIRCUITS
Examples of Nonlinear Devices

SABEUR LAFI
AMMAR KOUKI
JEAN BELZILE

ETS-RT - 2016-003

IMPLEMENTATION DETAILS OF A HARDWARE ABSTRACTION-BASED DESIGN METHOLODY FOR RADIOFREQUENCY CIRCUITS
Examples of Nonlinear Devices

DÉTAILS D'IMPLÉMENTATION D'UNE MÉTHODOLOGIE DE CONCEPTION DE CIRCUITS RADIOFRÉQUENCES BASÉE SUR L'ABSTRACTION MATÉRIELLE
Exemples de Circuits Non Linéaires

ETS TECHNICAL REPORT

SABEUR LAFI
AMMAR KOUKI
JEAN BELZILE

ELECTRICAL ENGINEERING DEPARTMENT

ÉCOLE DE TECHNOLOGIE SUPÉRIEURE
UNIVERSITÉ DU QUÉBEC

MONTRÉAL, MAY 18, 2016

ETS-RT - 2016-003

IMPLEMENTATION DETAILS OF A HARDWARE ABSTRACTION-BASED DESIGN METHOLODY FOR RADIOFREQUENCY CIRCUITS

Examples of Nonlinear Devices

SABEUR LAFI
AMMAR KOUKI
JEAN BELZILE
ELECTRICAL ENGINEERING DEPARTMENT
ÉCOLE DE TECHNOLOGIE SUPÉRIEURE

Electronic version of this technical report is available on the École de technologie supérieure web site (http://www.etsmtl.ca).

In order to request a paper copy, please contact :

Service de la bibliothèque
École de technologie supérieure
1100, rue Notre-Dame Ouest
Montréal (Québec)
H3C 1K3

Phone : (514) 396-8946
Fax : (514) 396-8633
Email : biblio@etsmtl.ca

ISBN 978-2-921145-85-5

Legal Deposit : Bibliothèque et Archives nationales du Québec, 2016
Legal Deposit : Library and Archives Canada, 2016

DÉTAILS D'IMPLÉMENTATION D'UNE MÉTHODOLOGIE DE CONCEPTION DE CIRCUITS RADIOFRÉQUENCES BASÉE SUR L'ABSTRACTION MATÉRIELLE
Exemples de Composants Non Linéaires

SABEUR LAFI
AMMAR KOUKI
JEAN BELZILE

SOMMAIRE

L'émergence de nouvelles applications et services mobiles contribuent à la hausse des attentes des utilisateurs en ce qui a trait aux performances des systèmes de radiocommunications. Toutefois, la conception de tels systèmes devient de plus en plus difficile à cause de la multitude de normes en usage, l'encombrement du spectre électromagnétique et l'hostilité accrue des environnements d'exploitation. Afin de faire face à ces exigences, des améliorations remarquables des approches de conception des systèmes radiofréquences doivent avoir le jour. À cet effet, plusieurs défis de conception tels que les problèmes de productivité, collaboration entre concepteurs, automatisation, conception et réutilisation des solutions ainsi que l'insertion de nouvelles technologies doivent avoir une attention particulière.

Dans l'optique de contribuer à la résolution de ces problèmes de conception, nous avons proposé dans des publications scientifiques récentes une nouvelle méthodologie de conception des circuits radiofréquences basée sur l'abstraction matérielle. Nous avons particulièrement détaillé les piliers de cette approche se basant sur un cycle de conception de cinq étapes qui est conçue autour d'une structure de données multidimensionnelle, la matrice Q, et à laquelle est projetée une stratégie d'abstraction. Nous avons choisi de valider la méthodologie proposée par le biais de cas d'études correspondant à des applications réelles. Dans ce rapport, nous détaillons le processus de conception de composants d'atténuation de puissance et de translation de fréquences. Deux scénarios différents et les étapes de conception sont particulièrement soulignés.

Mots clefs: Conception radiofréquence, abstraction matérielle, matrice Q, validation.

IMPLEMENTATION DETAILS OF A HARDWARE ABSTRACTION-BASED DESIGN METHOLODY FOR RADIOFREQUENCY CIRCUITS
Examples of Nonlinear Devices

SABEUR LAFI
AMMAR KOUKI
JEAN BELZILE

ABSTRACT

The emergence of new applications and services raises consumer expectations regarding future radio systems' performance. However, radio design is becoming more challenging due to multi-standard functionality, spectrum crowdedness and harsh operating environments. In order to keep pace with the emerging requirements, notable enhancements in radiofrequency design approaches are required. At this regard, several design challenges should be addressed especially in terms of productivity, design collaboration, automation and reuse as well as ensuring better technology insertion.

To tackle all these challenges, we have proposed in recent research publications a proposal of a new radiofrequency design framework based on hardware abstraction. We have particularly detailed its key foundations: a five-step design scheme that is streamlined to a novel abstraction strategy and built around a multidimensional data structure, namely the Q-matrix. We have undertaken the validation process of the proposed framework through selected design case studies corresponding to real-world applications. In this technical report, we present in some detail the framework validation results for the design of power attenuation and radiofrequency translation devices. Two scenarios were investigated and the overall design process was detailed.

Keywords: radiofrequency design, hardware abstraction, Q-matrix, framework validation.

TABLE OF CONTENTS

SOMMAIRE IV

ABSTRACT V

TABLE OF CONTENTS VI

LIST OF TABLES VIII

LIST OF FIGURES X

1 CASE STUDY I: POWER ATTENUATION DEVICE 13

- 1.1 Introduction 13
- 1.2 Specifications 13
- 1.3 Functional Description: SysML requirements and platform-independent models 13
- 1.4 Analysis: Coherence verification 14
- 1.5 Analysis: PSM generation 20
- 1.6 Synthesis: Technology mapping 23
- 1.7 Synthesis: PM generation 28
- 1.8 Using Q-matrix for noise data storage 34

2 CASE STUDY II: FREQUENCY TRANSLATION DEVICE 44

- 2.1 Introduction 44
- 2.2 Specifications 44
- 2.3 Functional Description: SysML requirements and platform-independent models 44
- 2.4 Analysis: Coherence verification 48
- 2.5 Analysis: PIM-level granularity refinement and simulation 56
- 2.6 Analysis: PSM generation 58
- 2.7 Synthesis: technology mapping 68
- 2.8 Synthesis: PM generation 73

REFERENCES 78

APPENDIXES 79

APPENDIX A SUMMARY OF EQUATIONS AND FORMULAS USED IN CASE STUDIES 80

LIST OF TABLES

Table 1.1 Typical specifications of a 3-dB RF attenuator 13

Table 1.2 List of values of « Attenuator » block...18

Table 1.3 List of values of each « Port » block...19

Table 1.4 Relationships between attenuator parameters given in Figure 1.5..................23

Table 1.5 Attenuator integrity control rules...24

Table 1.6 PIM-to-PSM transformation for T and Π resistive attenuators.......................26

Table 1.7 Values of resistors for T and Π attenuators...27

Table 1.8 T attenuator initial resistors...37

Table 1.9 Π attenuator initial resistors..37

Table 1.10 T attenuator alternative resistors..38

Table 1.11 Π attenuator alternative resistors..39

Table 1.12 Form factor of initial and refined PIMs for both T and Π attenuators...........40

Table 1.13 Intra-view transformation used for the attenuators' PSM granularity refinement..40

Table 2.1 Mixer specifications..45

Table 2.2 List of mixer value properties as presented in the corresponding bdds...........50

Table 2.3 List of mixer port value properties as enumerated in the SysML models 51

Table 2.4 Mixer PIM-level design constraints rules 54

Table 2.5 Common relationships between mixer parameters given in Figure 2.8...........56

Table 2.6 Mixer integrity control rules 57

Table 2.7 Passive diode mixer PIM-to-PSM transformation..59

Table 2.8 Rat-race Mixer PIM to PSM transformation 60

Table 2.9 Generated PSMs: Summary of both mixer PSMs performance characteristics 67

Table 2.10 Generated PSMs: Objective function calculations for each filter prototype 67

Table 2.11 Properties of the synthesized rat-race microstrip sections (RO3006 substrate) 69

Table 2.12 List of suitable diode parts found in the technology library 69

Table 2.13 List of inductor parts found in the technology library during automated technology mapping 72

Table 2.14 List of capacitor parts found in the technology library during automated technology mapping 72

Table 2.15 Comparison of the performance of the three PSM prototypes 73

Table 2.16 Technology mapped PSM: Objective function calculations for each rat-race mixer prototype 73

LIST OF FIGURES

Figure 1.1 Attenuator functional description overview: RM/PIM packages 15

Figure 1.2 The detailed attenuator's block definition diagram 17

Figure 1.3 The main attenuator requirements depicted in the associated SysML diagram 20

Figure 1.4 Value Types package 21

Figure 1.5 Attenuator's parameters relationships graph 22

Figure 1.6 Attenuator coherence verification report 25

Figure 1.7 Attenuator black-box model frequency response 26

Figure 1.8 A comparison between the T and Π attenuators in terms of frequency response and noise levels (at the end of step 1 of the PIM-to-PSM transformation) 29

Figure 1.9 PIM-to-PSM transformation: (a) T and (b) Π attenuators 32

Figure 1.10 A comparison between the T and Π attenuators in terms of frequency response and noise levels (at the end of step 2 of the PIM-to-PSM transformation) 32

Figure 1.11 Technology mapping: (a) T and (b) Π attenuators 33

Figure 1.12 A comparison between the T and Π attenuators in terms of frequency response and noise levels (initial technology mapping)................................35

Figure 1.13 Intra-view transformation: (a) series (b) shunt 35

Figure 1.14 A comparison between the T and Π attenuators in terms of frequency response and noise levels (after granularity refinement) 36

Figure 1.15 Resulting PM: (a) T and (b) Π attenuator layouts 38

Figure 1.16 Resulting PM after granularity refinement: (a) T and (b) Π attenuator layouts 39

Figure 1.17 A comparison between the T and Π attenuators in terms of frequency response and noise levels (Final PM 1)..41

Figure 1.18 A comparison between the T and Π attenuators in terms of frequency response and noise levels (final PM after granularity refinement) 42

Figure 1.19 Noise data is supported in the Qmatrix through metadata............................43

Figure 2.1 A mixer makes a frequency translation 44

Figure 2.2 Mixer package diagram 46

Figure 2.3 Three-port network detailed block definition diagram..................................47

Figure 2.4 Mixer is a nonlinear frequency conversion device (Figure 2.3 cont'd)..........49

Figure 2.5 Summary of mixer requirements 52

Figure 2.6 Coherence rules: PIM-level design rules...53

Figure 2.7 Mixer value types package 54

Figure 2.8 Mixer parameters relationships graph 55

Figure 2.9 Mixer coherence verification report 58

Figure 2.10 Black-box model frequency response..60

Figure 2.11 PSM topology: passive (a) single-ended diode and (b) rat-race mixer 62

Figure 2.12 Voltage waves: (a) Single-ended and (b) rat-race diode mixer 63

Figure 2.13 Output versus input power and (b) conversion gain of both mixers 64

Figure 2.14 Output Spectrum: (a) Single-ended and (b) rat-race diode mixer 65

Figure 2.15 Output Third-Intercept Point: (a) Single-ended and (b) rat-race diode mixer..66

Figure 2.16 Technology mapping results for (a) capacitor and (b) inductor elements...71

Figure 2.17 Conversion gain of the generated PSMs after technology mapping.............74

Figure 2.18 Platform Model: Layout of the final rat-race mixer 75

Figure 2.19 The Q-matrix stores both linear and nonlinear data 76

Figure 2.20 The Q-matrix stores data that can be interpreted in different ways..............77

1 CASE STUDY I: POWER ATTENUATION DEVICE

1.1 Introduction

In this first case study, we undertake the design of a power attenuation device, a radiofrequency (RF) attenuator. We attempt also how to use the proposed framework for concurrent design. To this end, we develop in parallel two prototypes that are optimized, validated and compared throughout the design cycle.

1.2 Specifications

On the contrary to filters, an attenuator is a radiofrequency device that degrades intentionally the signal level in a wide frequency band and beyond. Various types of attenuators (e.g., fixed, switched or continuously variable) are used for either circuit protection from high-signal levels or to provide accurate impedance matching. Among the key properties of an attenuator, we count the attenuation level, frequency range to which that attenuation applies and the input / output impedances. For this case study, we consider the specifications listed in Table 1.1.

Table 1.1 Typical specifications of a 3-dB RF attenuator

Attenuation level (dB)	3.0
Frequency Range (MHz)	0 – 2000 MHz
Noise Figure (dB)	< 0.5
Termination Impedance (ohm)	50
Other Requirements	Small form factor

1.3 Functional Description: SysML requirements and platform-independent models

The SysML diagrams used for the attenuator's functional description are similar to those elaborated for bandpass and lowpass filters. The package diagram of Figure 1.1 depicts the main constituents of the functional description:

- Attenuator definition: this package defines the functional and structural aspects of the attenuator. Its general organization is inspired from the RF stereotypes presented in the "SysML profile for RF devices" (Lafi, 2016b). For example, the bdd of Figure 1.2 shows the properties of the attenuator block as well as the hierarchy of blocks related to it. Thus, an attenuator inherits the properties of the « Power Attenuation and Matching Device », which is itself a linear two-port network. The complete list of attenuator values are given in Table 1.2. The values of « Port » block are provided separately in Table 1.3;
- Attenuator requirements: as shown in Figure 1.3, the requirements related to the attenuator design are similar to those depicted in presented in the "SysML profile for RF devices" (Lafi, 2016b). In this case, the attenuator requirements can be subdivided into two major categories: performance and form factor. The first includes the required attenuation level and its associated frequency range. The second summarizes the requirements related to the form and size of the device;
- Attenuator coherence rules: the functional description of the attenuator is submitted in the next design stage, namely « Analysis ». The related rules are assembled in « Coherence Rules » package (see Figure 1.1) that is detailed in the next design stage;
- Value types: this package defines the units, constants and other modeling artifacts used in the other packages. As illustrated in Figure 1.4, the units used in attenuator definition bdds to define values' types are reported.

It is worth noting that the SysML diagrams shown in this section are part of the attenuator functional description but not exhaustive and presented for illustration purposes only.

1.4 Analysis: Coherence verification

The attenuator's functional description should be submitted to coherence verification at this step in order to figure out any eventual errors. The set of rules used for this process is composed of electrical consistence and integrity controls rules. No PIM-level design constraints' rules are defined for this case study.

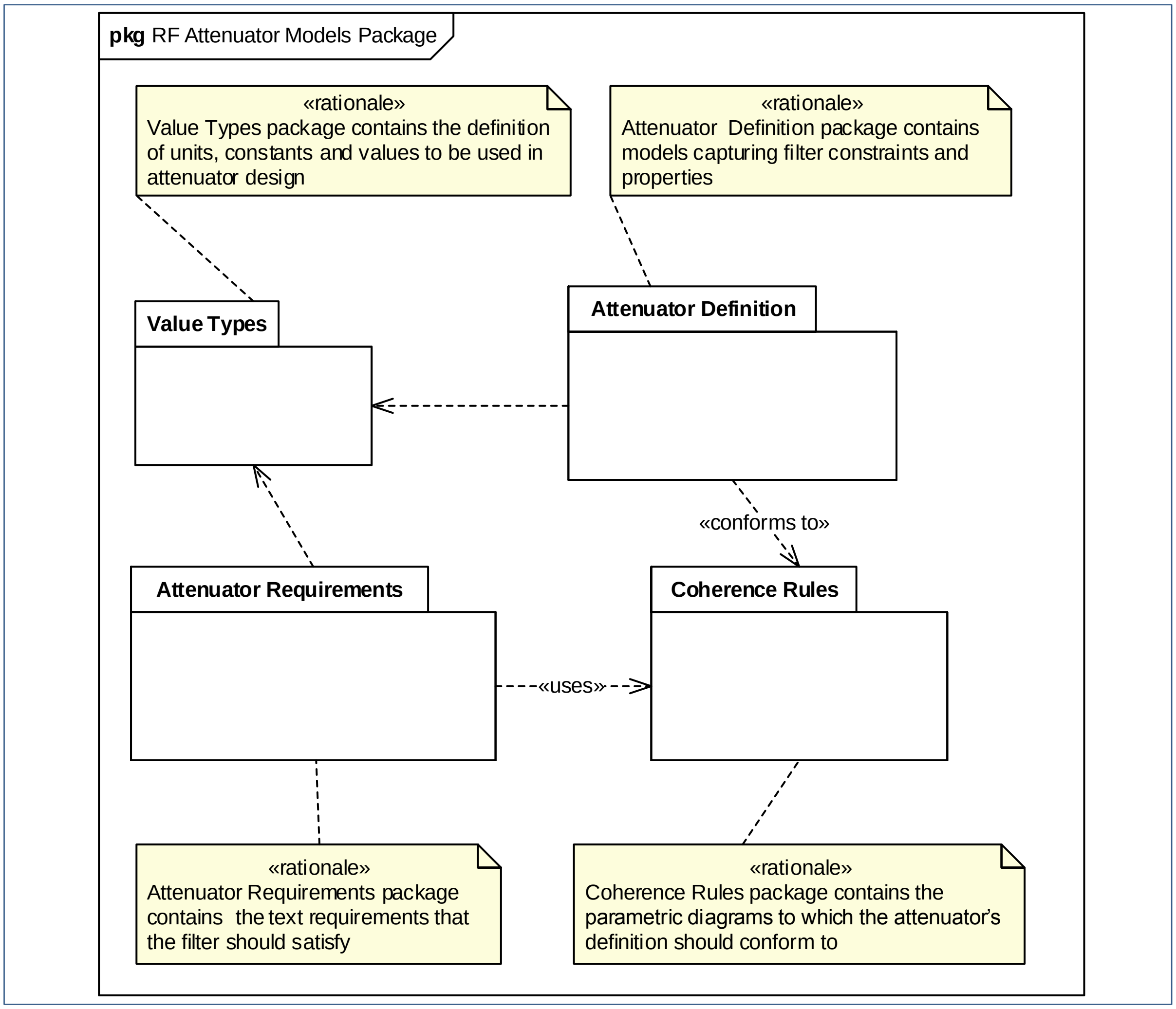

Figure 1.1 Attenuator functional description overview: RM/PIM packages

– The electrical consistence rules: the goal of these rules is to check the coherence between the various attenuator value properties. We defined a set of rules based on the equations of Table 1.4. These rules are mapped to the attenuator parameters as depicted in Figure 1.5;

- The integrity controls rules: the attenuator value properties must be defined within a predefined range. The integrity rules listed in Table 1.5 check if each value property is unusually sized.

Using a dedicated algorithm, the attenuator's functional description is checked against the 33 rules (i.e., eleven for electrical consistence and thirty two for integrity control tests). The resulting coherence verification report is depicted in Figure 1.6.

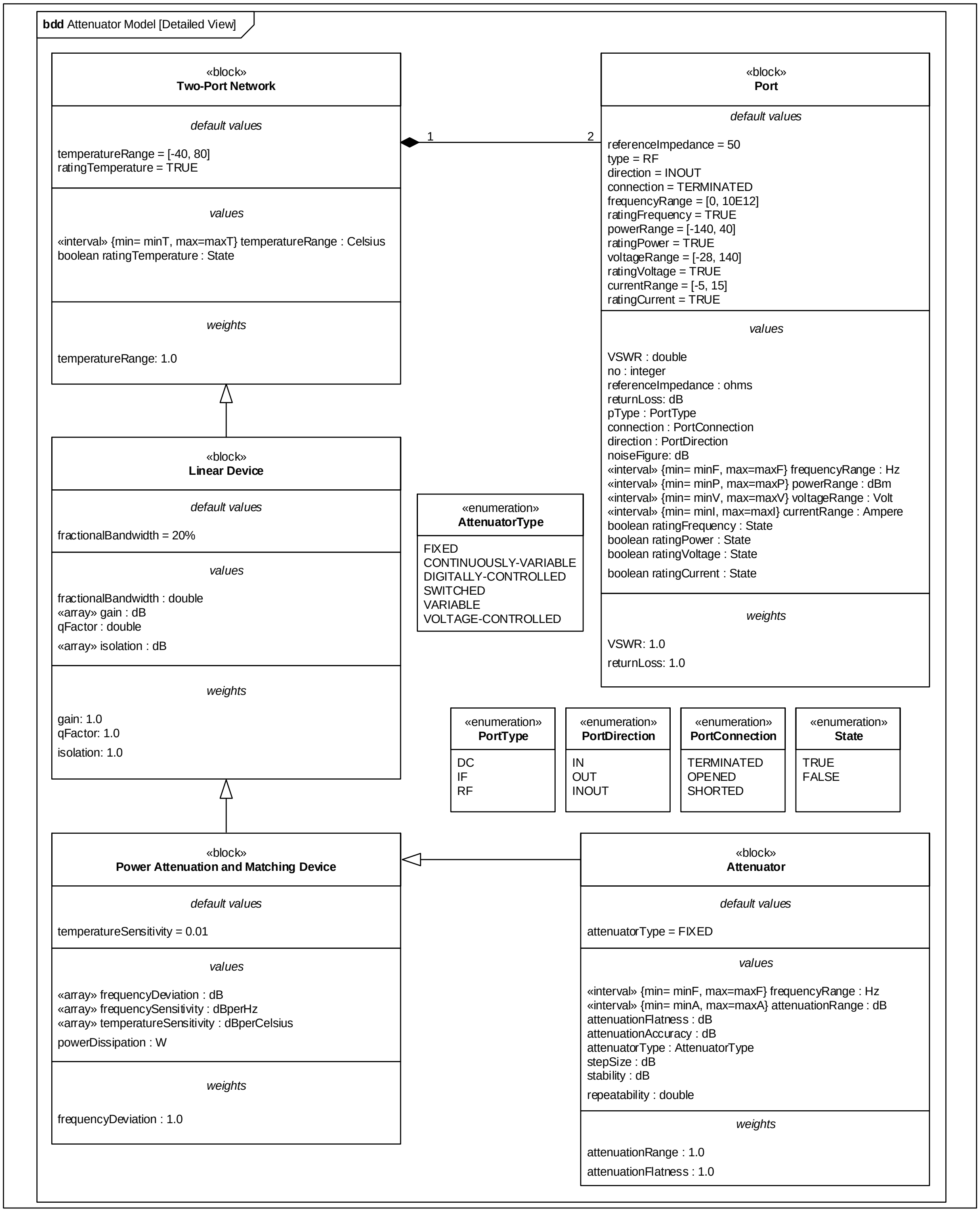

Figure 1.2 The detailed attenuator's block definition diagram

Table 1.2 List of values of « Attenuator » block

Parameter Value	Type	Default Value	Remarks	Specifications Value
temperatureRange	interval (Celsius)	[-40, 80]		
ratingTemperature	Boolean	TRUE	TRUE FALSE	
portList	Object (Port)			
portsNo	integer	2		
fractionalBandwidth	double	20%		ignored
gain	array (dB)			Overridden by *attenuationRange*
qFactor	double			
isolation	dB			Overridden by *attenuationRange*
temperatureSensitivity	dBperCelsius	0.01		
frequencyDeviation	dB			
frequencySensitivity	dBperHz			
powerDissipation	W			
attenuatorType	AttenuatorType	FIXED	FIXED CONTINUOUSLY-VARIABLE DIGITALLY-CONTROLLED SWITCHED VARIABLE VOLTAGE-CONTROLLED	
frequencyRange	Hz			min.: 0 max.: 2000 MHz
attenuationRange	dB			3.0
attenuationFlatness	dB			
attenuationAccuracy	dB			
stepSize	dB			

stability	dB			
repeatability	double			

Table 1.3 List of values of each « Port » block

Parameter Value	**Type**	**Default Value**	**Remarks**	**Specifications Value**
VSWR	double			
no	integer			1 (2)
referenceImpedance	double (ohms)	50.0		50.0 (50.0)
returnLoss	dB			
noiseFigure	dB			max. 0.5 (max. 05)
pType	PortType	RF	DC IF RF	
direction	PortDirection	INOUT	IN OUT INOUT	
connection	PortConnection	TERMINATED	TERMINATED OPENED SHORTED	
frequencyRange	interval (Hz)	[0, 10E12]		
ratingFrequency	Boolean	TRUE	TRUE FALSE	
powerRange	interval (dBm)	[-140, 40]		
ratingPower	Boolean	TRUE	TRUE FALSE	
voltageRange	interval (volts)	[-28, 140]		
ratingVoltage	Boolean	TRUE	TRUE FALSE	
currentRange	interval (amperes)	[-5, 15]		
ratingCurrent	Boolean	TRUE	TRUE FALSE	

After coherence verification comes design exploration where a black-box model is associated to the functional description in the purpose of finding out a suitable design solution. The black-box model is given by the equation (A-1, p. 80) of APPENDIX A. A first assessment of the black-box model results in the curves given in Figure 1.7.

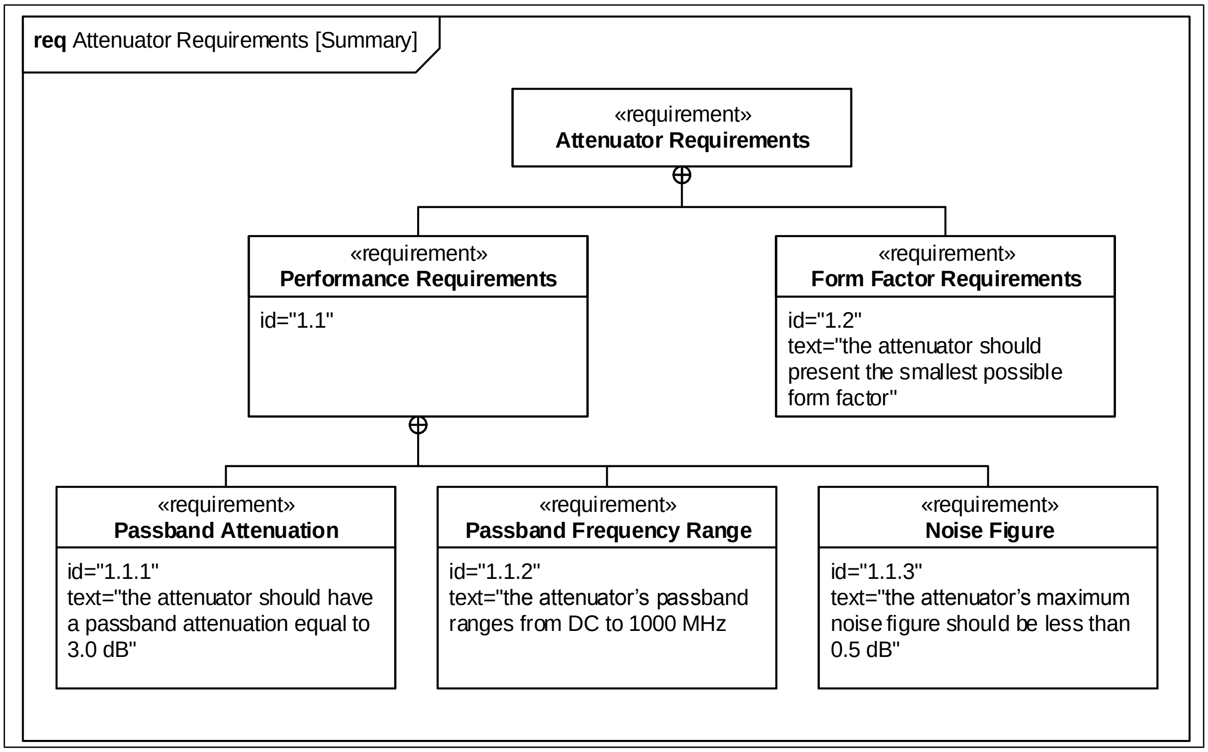

Figure 1.3 The main attenuator requirements depicted in the associated SysML diagram

1.5 Analysis: PSM generation

Given the satisfactory performance of the black-box model, no refinement is required. The following task is the PSM generation using a relevant PIM-to-PSM transformation. In this case study, we present a transformation that results in two different prototypes of the PSM. This is because we aim at testing the concurrent design using the proposed framework. The PIM-to-PSM transformation of Table 1.6 develops two PSMs (i.e., T- and π-pad symmetric attenuators). Each PSM is implemented in two successive steps:

1. Step 1: Calculation of T- (respectively π-pad) resistive elements

The first transformation step consists of the computation of resistive elements corresponding to the T-pad (respectively π-pad) attenuator. The values of these elements (already listed in Table 1.7) are structured into a T (respectively Π) attenuator topology. Given the topology and the resistive elements of each attenuator, it becomes possible to simulate and compare the frequency response and the noise levels in both PSMs (see Figure 1.8). It is worth noting that the resistive elements are ideal and no physical connections between them are considered.

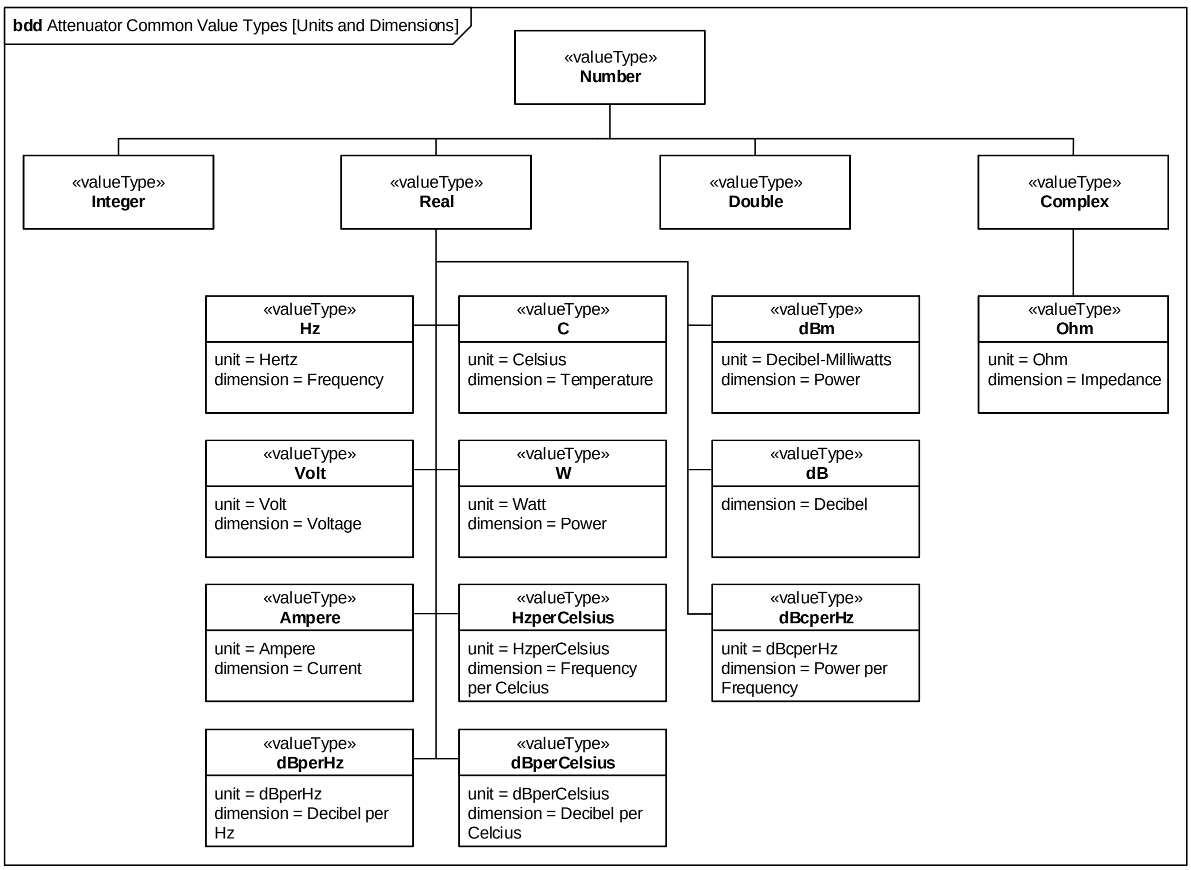

Figure 1.4 Value Types package

2. Step 2: Synthesis of transmission lines and circuit topology

The attenuator topologies resulting from the previous step cannot be physically implemented because the resistive elements are not connected using physical structures. That is why transmission lines are synthesized in the second step of the transformation. Depending on topology, the resistive elements are connected together using ideal transmission line sections (see Figure 1.9.a and Figure 1.9.b). The performance of both attenuators is depicted in Figure 1.10. As expected, a slight degradation in frequency response as well as an increase of noise levels for both topologies are observed due to the effects of transmission-line sections.

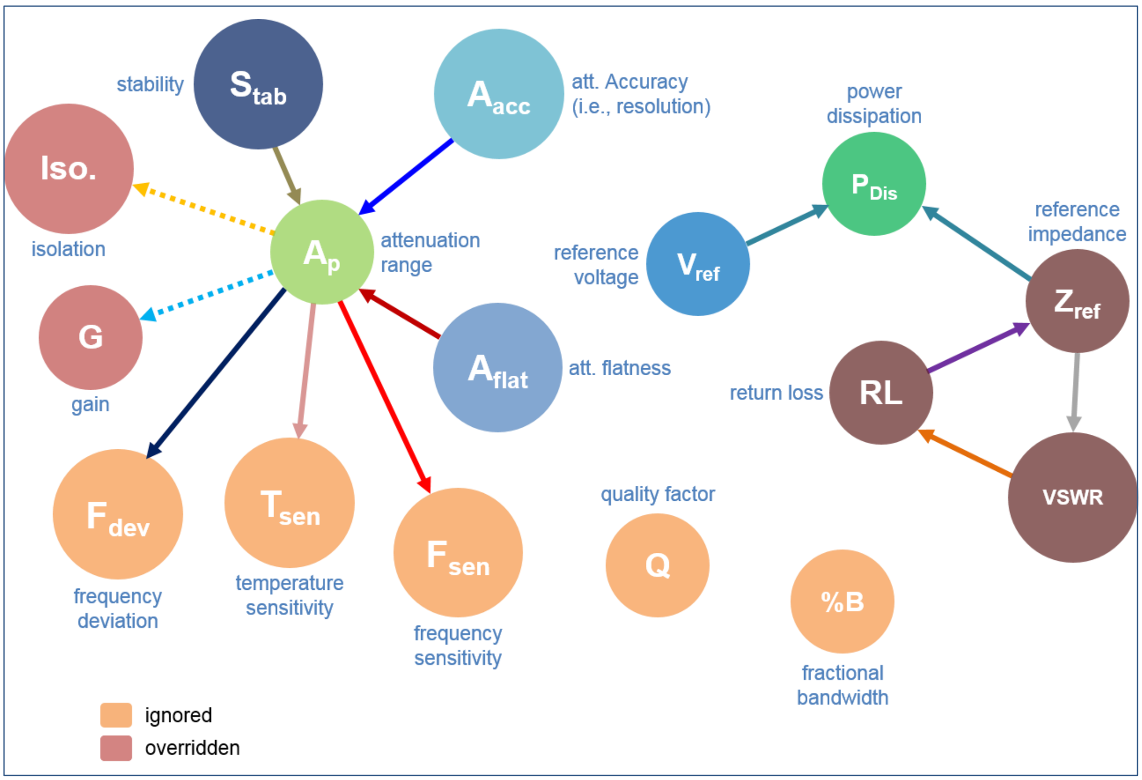

Figure 1.5 Attenuator's parameters relationships graph

1.6 Synthesis: Technology mapping

The PIM-to-PSM transformation resulted in two PSMs (i.e., T- and π-pad symmetric attenuators). In this step, we do not submit these PSMs to PSM-level granularity refinement because the obtained frequency response for both prototypes is relatively satisfactory (see Figure 1.10). The components used so far are ideal. In technology mapping, we search the available technology libraries in order to augment both PSMs with detailed technology information. For this purpose, we proceed in two steps:

- Selection of resistors: since the available resistors do not cover all resistance values, we select the closest values to each resistor in ideal PSMs. The selected resistors for T-pad (respectively π-pad) attenuator are reported in Table 1.8 (respectively 1.9);
- Synthesis of transmission-line sections: the sections we added in the second step of the PIM-to-PSM transformation in order to physically connect the resistors should be implemented. To do so, we use the properties of RO3006 substrate (see Table A.1) to synthesize each transmission line section. The width (respectively length) of each section is 35.980472 mil (respectively 39.238622 mil) when $\beta l = E_i = 5°$, $Z_{ci} = 50\ \Omega$ and $F_i = 1$ GHz. The technology-mapped T-pad (respectively π-pad) attenuator is depicted in Figure 1.11.a (respectively Figure 1.11.b).

Table 1.4 Relationships between attenuator parameters given in Figure 1.5

Arrow Color	Mathematical Relationship	Parameter
● (red)	$A_{flat} = \max(A_p) - \min(A_p)$	Attenuation flatness
● (blue)	$A_{acc} = average(A_p^{specified}) - average(A_p^{measured})$	Attenuation accuracy
● (olive)	$S_{tab} = average(A_p^{specified}) - average(A_p^{measured})\big\|_{Scale}$ $Scale \in \{T, F, P, t\}$	Stability
● (teal)	$P_{dissipated} = \frac{(V_{ref})^2}{Z_{ref}}$	Dissipated power
● (pink)	$T_{sen} = average\left(A_p\big\|_{T+\Delta T} - A_p\big\|_{T}\right)$	Temperature sensitivity

●	$F_{sen} = average\left(A_p\big\vert_{F+\Delta F} - A_p\big\vert_{F}\right)$	Frequency sensitivity
●	$F_{dev} = A_p$	Frequency deviation
●	$VSWR = \dfrac{10^{\frac{RL}{20}} + 1}{10^{\frac{RL}{20}} - 1}$	Voltage Standing Wave Ratio
●	$RL = \dfrac{Z_L - Z_S}{Z_L + Z_S}$	Return loss
●	$A_p = isolation$	Attenuation range overrides Isolation property
●	$R = G$	Attenuation range overrides Gain property

Table 1.5 Attenuator integrity control rules

No.	**Rule**	**if test fails**
I.1	$-80 \leq \text{temperatureRange} \leq 100$	Error or/and Warning
I.2	$\text{ratingTemperatureRange} \in \{\text{TRUE,FALSE}\}$	Error
I.3	$1 \leq \text{VSWR} \leq 10$	Error or/and Warning
No.	**Rule**	**if test fails**
I.4	$\text{no} \in \mathbb{N}^*$	Error
I.5	$0 < Z_{ref} \leq 10^4$	Error or/and Warning
I.6	$0 < RL \leq 120$	Error or/and Warning
I.7	$\text{ptype} \in \{\text{DC,IF,RF}\}$	Error
I.8	$\text{connection} \in \{\text{TERMINATED,OPENED,SHORTED}\}$	Error
I.9	$\text{direction} \in \{\text{IN,OUT,INOUT}\}$	Error
I.10	$0 \leq \text{frequencyRange} \leq 10^{12}$	Error or/and Warning
I.11	$0 \leq \text{powerRange} \leq 160$	Error or/and Warning
I.12	$0 \leq \text{voltageRange} \leq 10^4$	Error or/and Warning
I.13	$0 \leq \text{currentRange} \leq 10^2$	Error or/and Warning
I.14	$\text{ratingFrequency} \in \{\text{TRUE,FALSE}\}$	Error
I.15	$\text{ratingPower} \in \{\text{TRUE,FALSE}\}$	Error

I.16	ratingVoltage ∈ {TRUE,FALSE}	Error
I.17	ratingCurrent ∈ {TRUE,FALSE}	Error
I.18	$0 \le \%B \le 1$	Error
I.19	$Q \in]0,\infty[$	Error or/and Warning
I.20	$0 \le$ frequencyDeviation ≤ 120	Error
I.21	$0 \le$ frequencySensitivity ≤ 120	Error or/and Warning
I.22	$0 \le$ temperatureSensitivity ≤ 120	Error or/and Warning
I.23	$0 \le$ powerDissipation ≤ 120	Error or/and Warning
I.24	$0 \le F_{min} \le 10^{12}$	Error or/and Warning
I.25	$0 \le F_{max} \le 10^{12}$	Error or/and Warning
I.26	$\forall$i, $0 \le$ attenuation[i] ≤ 120	Error or/and Warning
I.27	$0 \le$ attenuationFlatness ≤ 120	Error or/and Warning
I.28	$0 \le$ attenuationAccuracy ≤ 120	Error or/and Warning
I.29	attenuatorType ∈ {FIXED, CONTINUOUSLY-VARIABLE, DIGITALLY-CONTROLLED, SWITCHED, VARIABLE, VOLTAGE-CONTROLLED}	Error
I.30	$0 \le$ stepSize ≤ 120	Error or/and Warning
I.31	$0 \le$ stability ≤ 120	Error or/and Warning
I.32	$0 \le$ repeatability ≤ 120	Error or/and Warning

```
******** Coherence Verification Test ********
TARGET PIM: 2-GHz RESISTIVE SYMMETRIC ATTENUATOR (C:\Users\slafi\Documents\Design\2ghz_att.xml)

-> Electrical Consistence Rules (11 found)
    ........................................ PASS
-> PIM-level Design Constraints Rules (0 found)
    ........................................ N/A
-> Integrity Control Rules (32 found)
    ........................................ PASS
    Summary: (0) Warnings (0) Errors
```

Figure 1.6 Attenuator coherence verification report

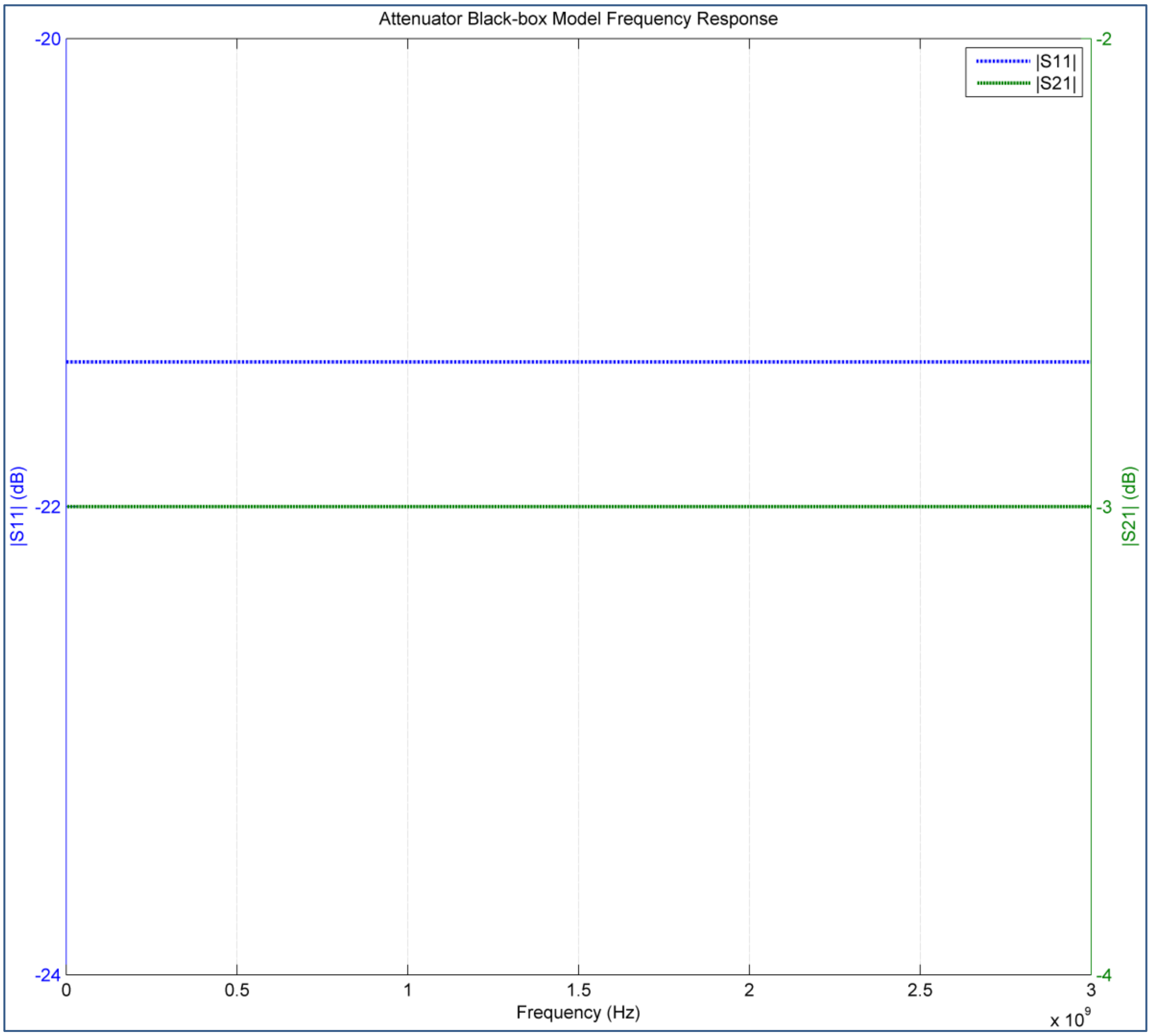

Figure 1.7 Attenuator black-box model frequency response

Table 1.6 PIM-to-PSM transformation for T and Π resistive attenuators

Step 1: Calculation of T- and π-pad elements
1.1. Calculate T-pad attenuator resistor values (R_k^T) (see equation (A-2) in APPENDIX A, p.80) 1.2. Calculate π-pad attenuator resistor values (R_k^π) (see equation (A-3) in APPENDIX A, p.81)
Step 2: Synthesis of transmission lines and circuit topology
2.1.a. For each series resistor:
Create topology depicted in Figure 1.9.a (step ❶).
2.2.b. For each parallel resistor:
Create topology depicted in Figure 1.9.b (step ❶).

2.3. For each transmission line:
Consider the properties given in the following:

$$\begin{cases} Z_{ci} = Z_{reference} \\ E_i = E_{default} \\ F_i = F_0 \\ A_i = A_{default} \end{cases}$$

where Z_{ci} is the characteristic impedance of the transmission line, E_i is its electrical length, F_i is the frequency at which the electrical length is calculated and A_i is the transmission line loss (in dB).

Table 1.7 Values of resistors for T and Π attenuators

Resistor value (Ω)	T Attenuator	Π Attenuator
R1	8.549868	292.40218
R2	141.926156	17.614794
R3	8.549868	292.40218

The performance assessment after technology mapping is depicted in Figure 1.8. The T-pad attenuator in terms of frequency response is better than its π-pad counterpart.

The resistors selected during technology mapping from a first technology library (see Table 1.8 and Table 1.9) use a 0603 package (1.63×0.81×0.46 mm). When searching a second technology library (i.e., Panasonic Components Library version 3.1), resistors packaging is provided in three different formats: 0201 (0.6×0.3×0.26 mm), 0402 (1.63×0.81×0.46 mm), and 0603. The smallest is 0201 but it is too small for handcrafted assembly. The packaging 0402 offers a better form factor. However, it is not possible to find out resistance values that approach better the ideal values given in Table 1.7 without combining two or more resistors. The second technology-mapping round resulted in the values listed in Table 1.10 and 1.11. For the T-pad attenuator, the best approximation of the ideal resistance value 141.9 Ω is the combined use of two resistors whose values are 120 Ω and 22 Ω respectively. Similarly, the π-pad attenuator requires a combination of two resistors from Panasonic library to approximate as much as possible the PSM ideal values (i.e., 270 Ω + 22 Ω → 292.4 Ω and 12 Ω + 5.6 Ω → 17.6 Ω).

The increase of the resistors number requires the PSM-level granularity to increase alike in order to keep the PSM coherent with its associated viewpoint. For this reason, it is mandatory to make a viewpoint change in order to increase the granularity level within the PSM. This takes place in the step of PSM-level granularity refinement using a relevant intra-view transformation. Thus, the design is sent back from « Technology Mapping » to « PSM-level Granularity Refinement » in order to change its granularity.

Using the intra-view transformation given in Table 1.13, both PSMs granularity level is altered. An additional resistor is added to the T-pad attenuator while three are added to its π-pad counterpart. After the use of resistors given in Table 1.10 and 1.11 as well as the synthesis of microstrip-line sections as explained above, the results of performance assessment of the new PSMs is depicted in Figure 1.14.

It is worth noting that the PSM-level granularity refinement process was launched in the bandpass filter case study due to the poor performance of the obtained design solution. In this case study, this process was provoked in the purpose of satisfying another requirement: small form factor. As explained in (Lafi, 2015), the granularity refinement process helps extending the limits of design space in a controlled fashion. Thus, it is always possible to proceed to granularity refinement to satisfy one or many design requirements and enhance the quality of the obtained design solution.

1.7 Synthesis: PM generation

The candidate design solutions whose frequency response is depicted in Figure 1.12 and 1.14 respectively are relatively satisfying. To move forward towards manufacturing stage, we use a PSM-to-PM transformation in order to generate the PM corresponding to each PSM.

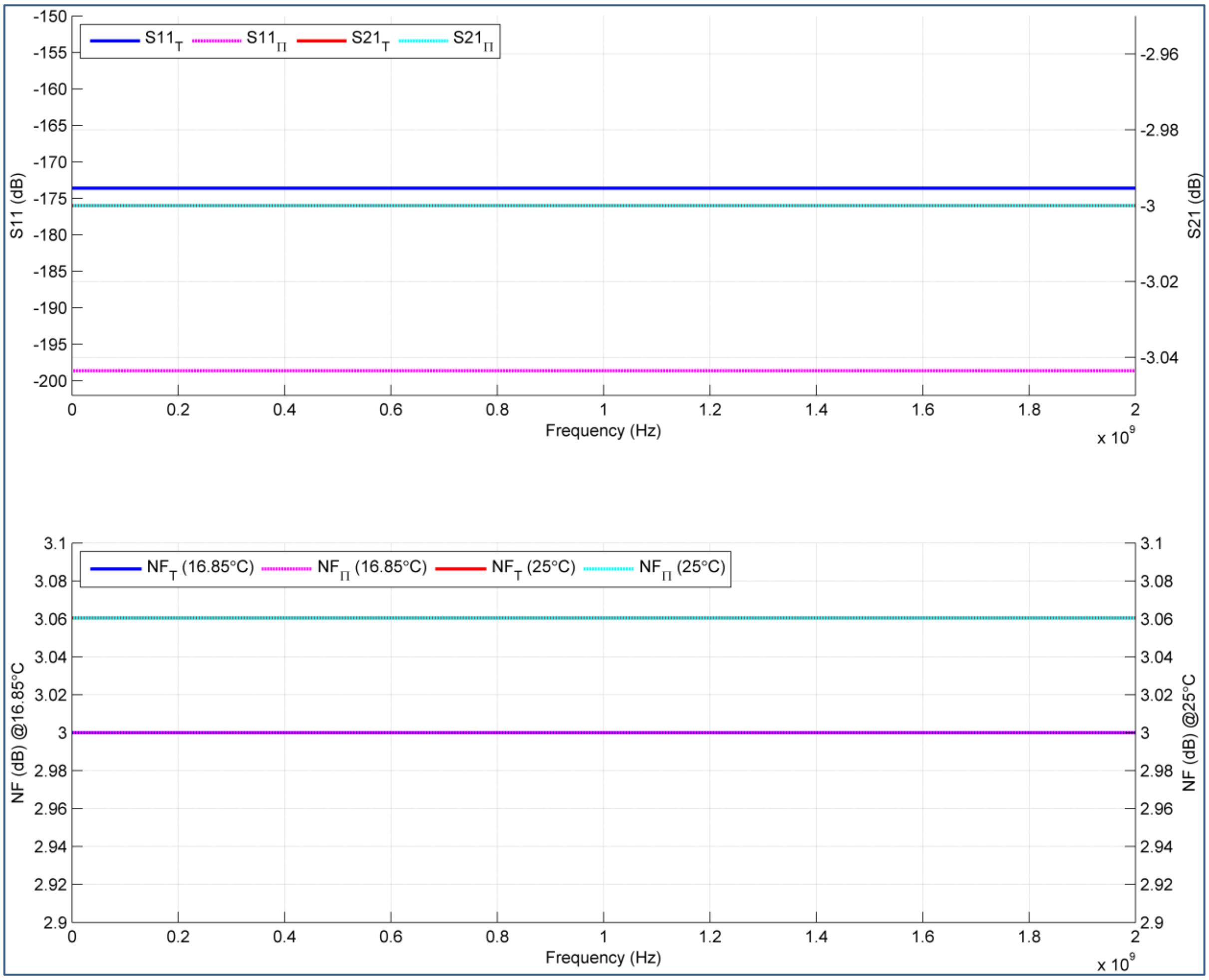

Figure 1.8 A comparison between the T and Π attenuators in terms of frequency response and noise levels (at the end of step 1 of the PIM-to-PSM transformation)

Using a commercial design package (i.e., ADS), we transform both PSMs into physical layouts. The PM corresponding to the PSM resulting from the initial technology mapping is illustrated in Figure 1.15. The PM corresponding to the PSM resulting from granularity refinement is depicted in Figure 1.16. It is trivial to note the effect of PSM-level granularity refinement between both PMs. For instance, an additional resistor (green colored) and an extra microstrip section (red colored) are observed in the T-pad attenuator of Figure 1.16.a which brings the total number of resistors to four (against three in the original attenuator PM illustrated in Figure 1.15.a). This observation is also valid to the π-pad attenuator PMs (Figure 1.16.b versus Figure 1.15.b). In addition, the frequency response of the generated PMs is illustrated in Figure 1.17 (original PSM) and 1.18 (PSM resulting from granularity refinement).

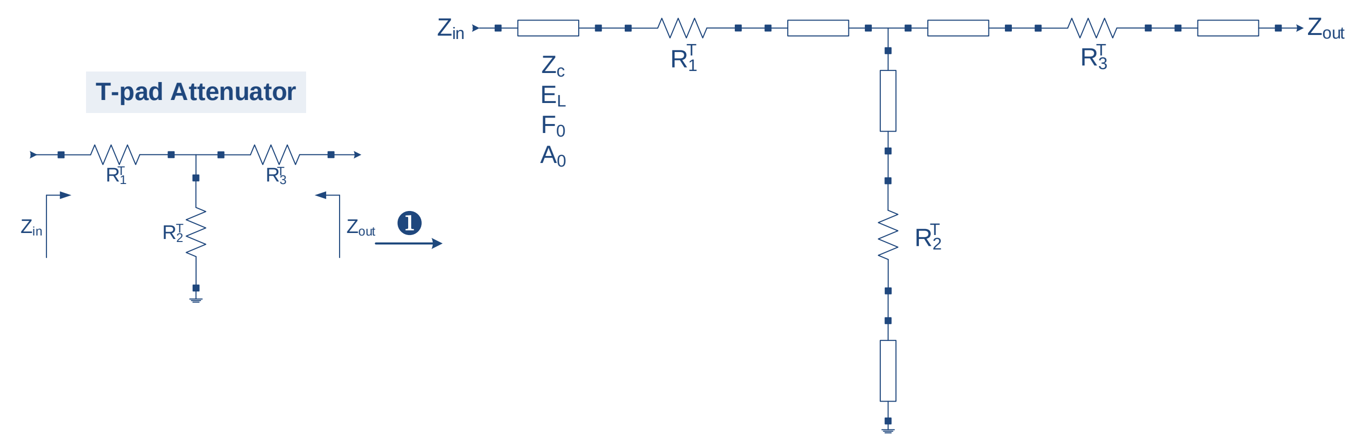
T-pad Attenuator
Zin
Zout
R1T
R2T
R3T
Zc
EL
F0
A0

(a)

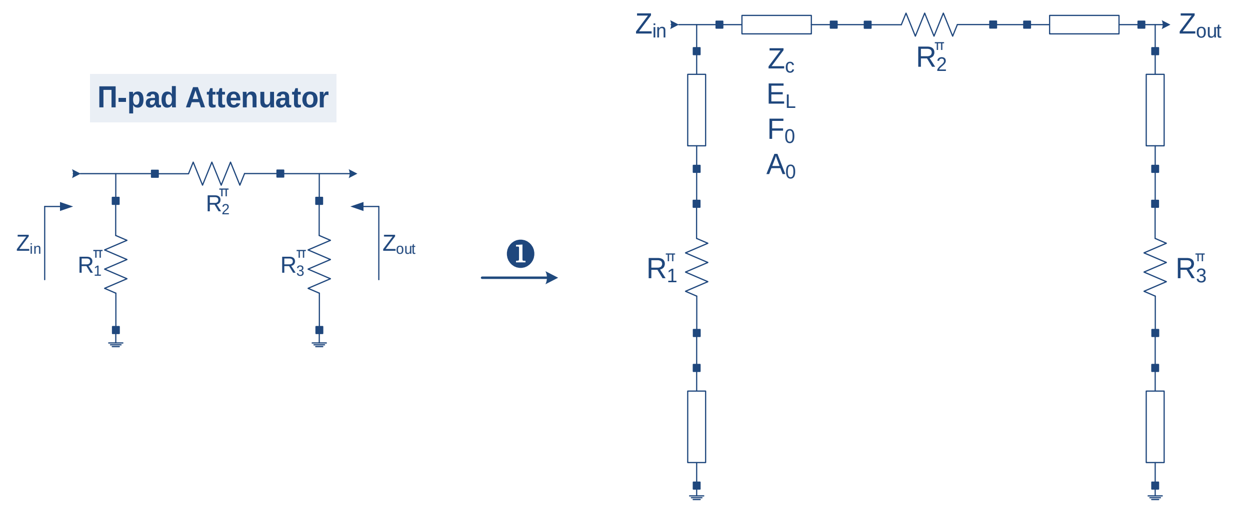
Π-pad Attenuator
Zin
Zout
R1π
R2π
R3π
Zc
EL
F0
A0

(b)

Figure 1.9 PIM-to-PSM transformation: (a) T and (b) Π attenuators

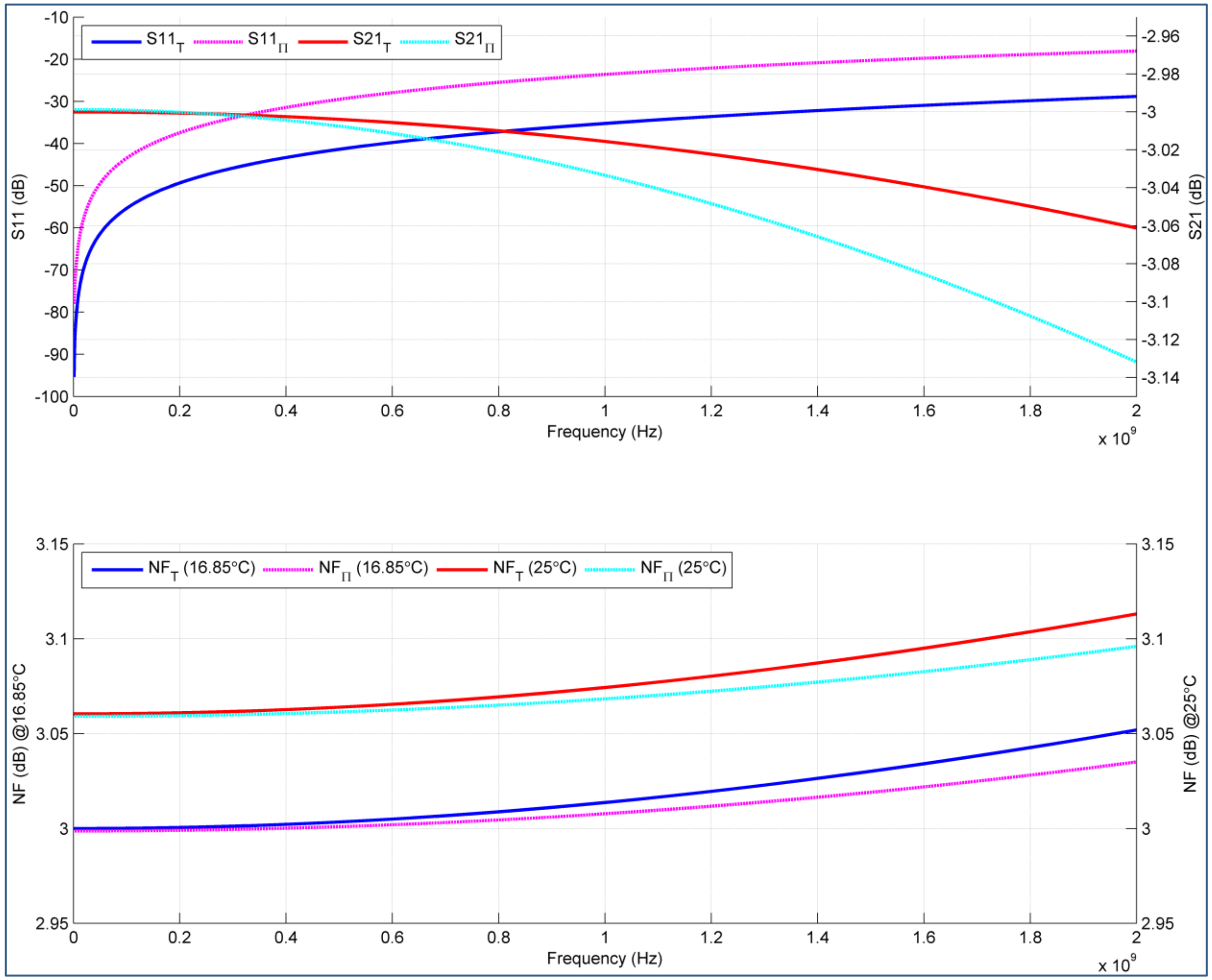

Figure 1.10 A comparison between the T and Π attenuators in terms of frequency response and noise levels (at the end of step 2 of the PIM-to-PSM transformation)

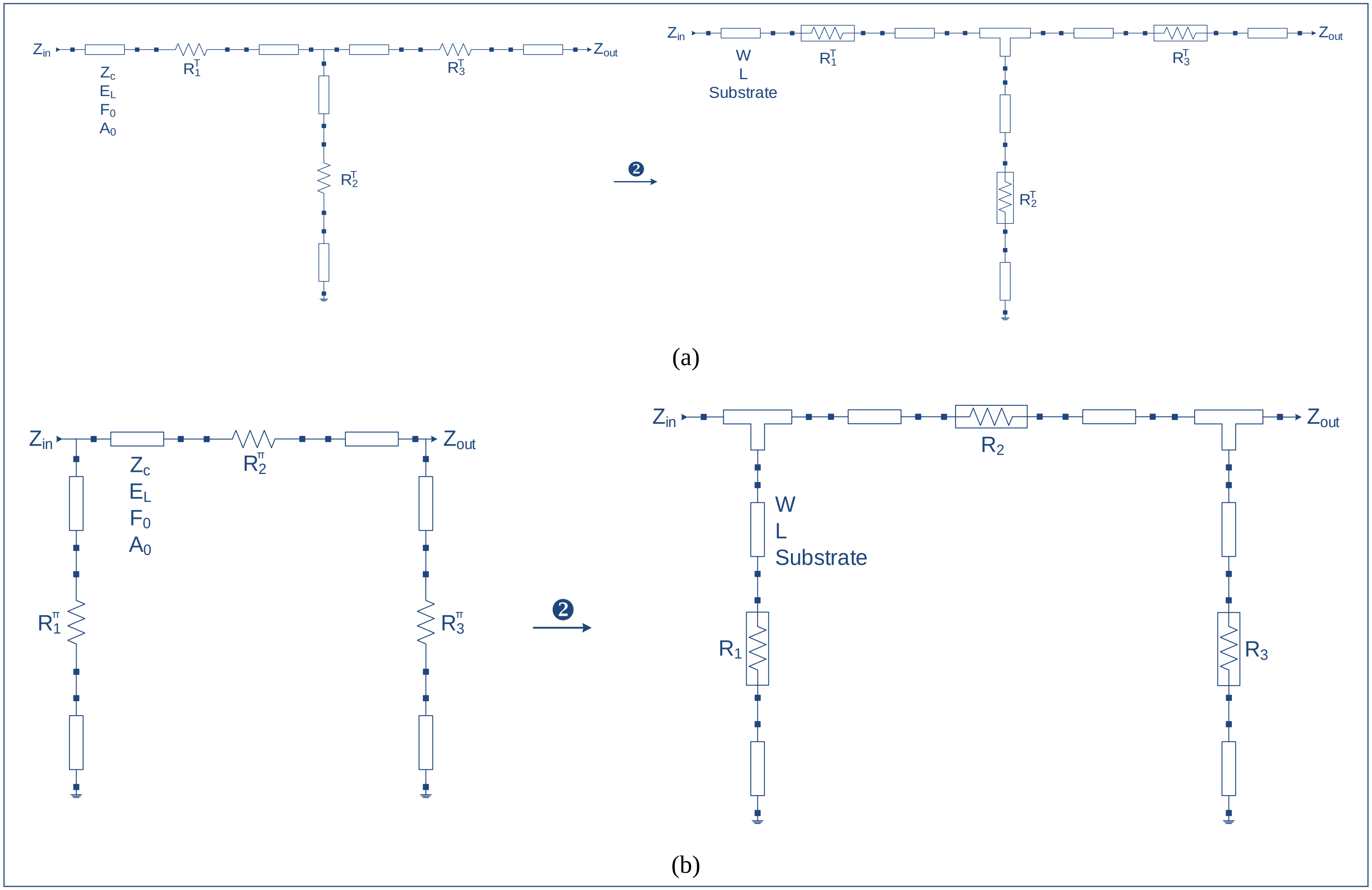

Figure 1.11 Technology mapping: (a) T and (b) Π attenuators

1.8 Using Q-matrix for noise data storage

In this case study, we chose to include the evaluation of the noise level in the performance assessment plan of each design solution. This information is part of electrical design data. However, it does not comply with the mathematical formalism of the Q-matrix (see section 1.3.1.c and equations (3.2)-(3.3) in (Lafi, 2015)). Thus, the noise data is not natively supported by the Q-matrix. Nevertheless, we used the Q-matrix XML data structure to include noise data as metadata. As illustrated in Figure 1.19, a dataset is created in metadata section where each noise point is included along with the relevant data. The frequency, temperature and data format are also provided.

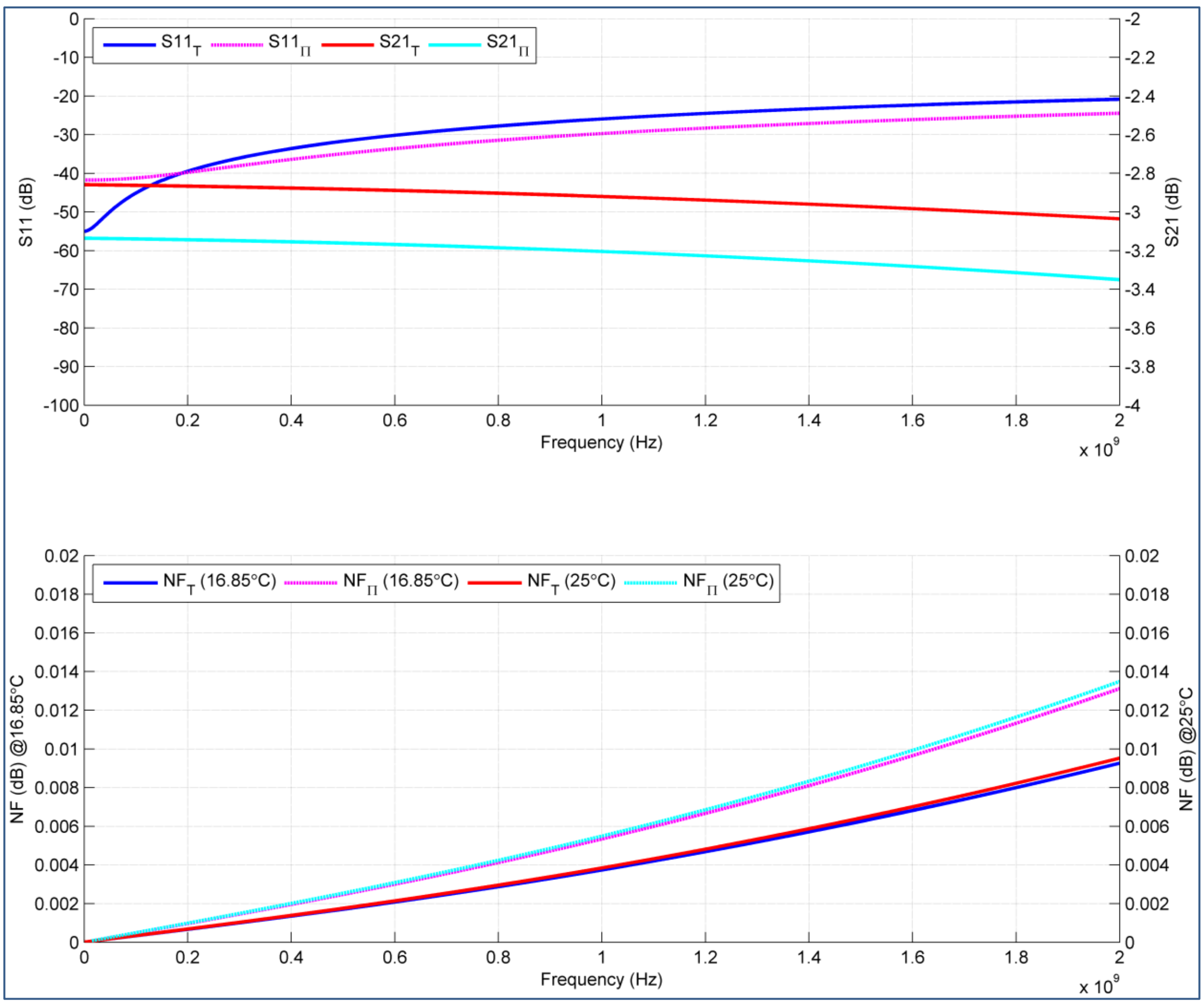

Figure 1.12 A comparison between the T and Π attenuators in terms of frequency response and noise levels (initial technology mapping)

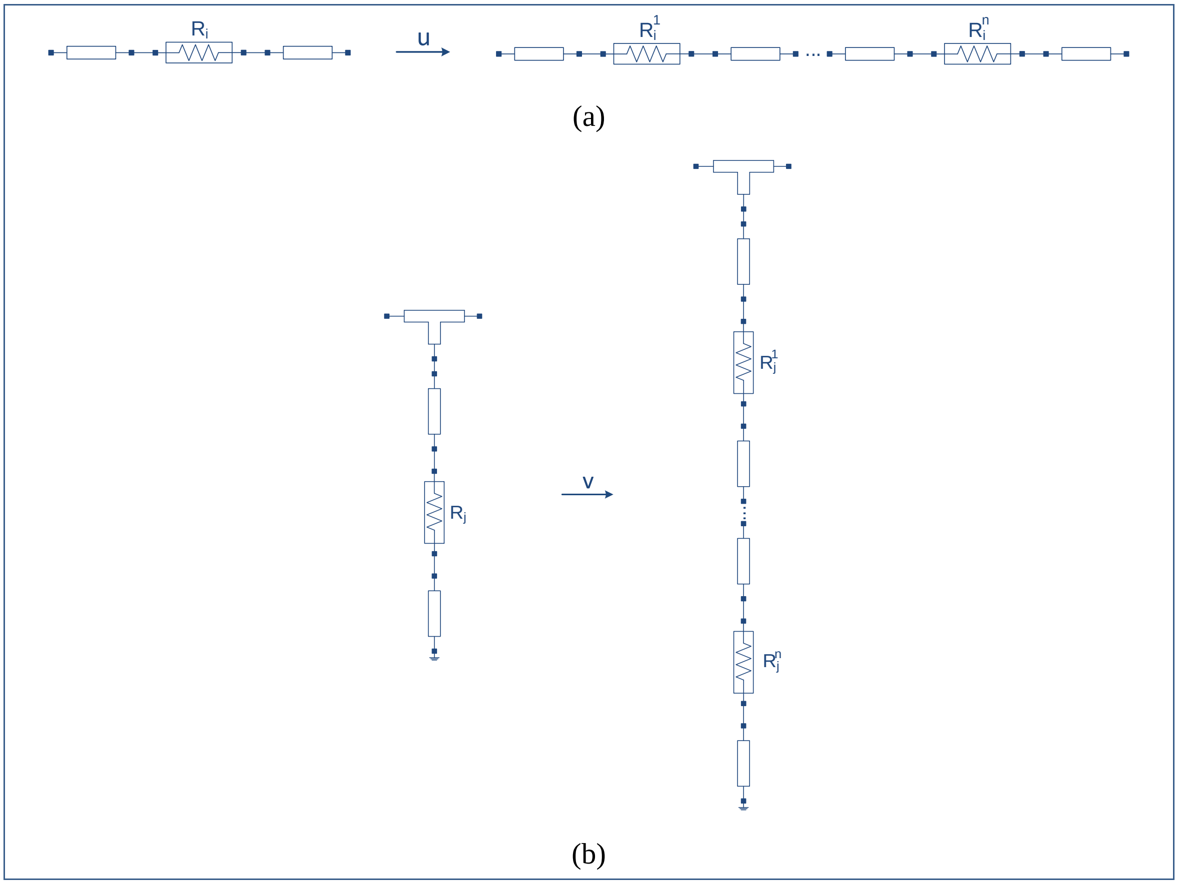

Figure 1.13 Intra-view transformation: (a) series (b) shunt

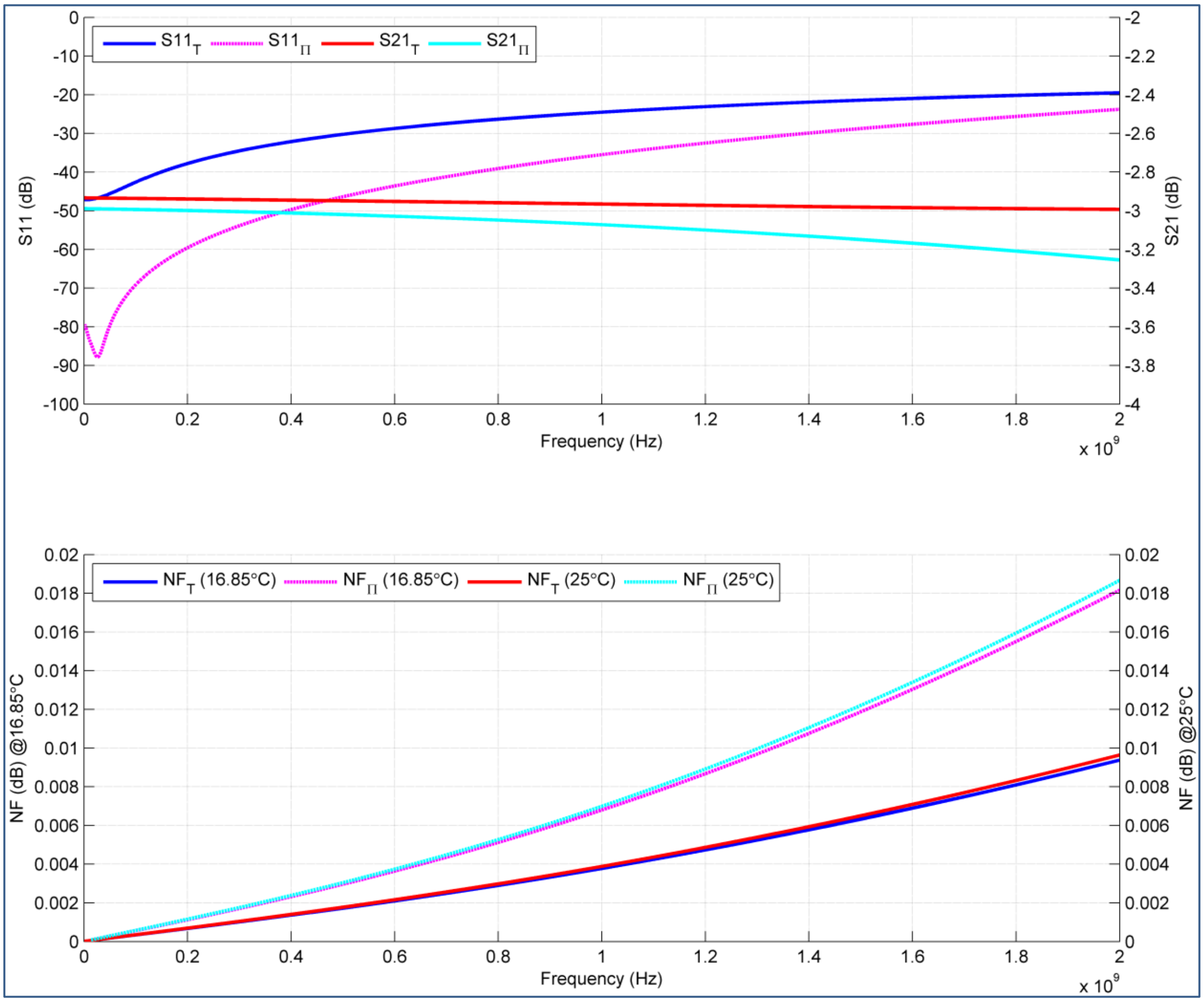

Figure 1.14 A comparison between the T and Π attenuators in terms of frequency response and noise levels (after granularity refinement)

Table 1.8 T attenuator initial resistors

Manufacturer Part Number	Resistance (Ω)	Tolerance	Power (W)	Package	Dimensions			Endurance
					Length	Width	Height	
PATT0603K8R45FGT1◊	8.45	±1%	0.15	0603	1.63	0.81	0.46	70°C, 1000h: ±(1% R + 0.05Ω) 70°C, 8000h: ±(2% R + 0.1Ω)
MCT06030D1400BP500♥	140	±0.1%	0.1	0603	1.55	0.85	0.55	
PAT0603E1400BST1◊	140	±0.1%	0.15	0603	1.63	0.81	0.46	

◊ Vishay Thin Film
♥ Vishay BC Components

Table 1.9 Π attenuator initial resistors

Manufacturer Part Number	Resistance (Ω)	Tolerance	Power (W)	Package	Dimensions (mm)			Endurance
					Length	Width	Height	
Y149617R6000C0W♠	17.6	±0.25%	0.15	1206	3.2	1.57	0.64	70°C, 1000h: ±(0.05% R + 0.01Ω) 70°C, 8000h: ±(0.1% R + 0.02Ω)
TNPW060317R4BEEN✦	17.4	±0.1%	0.1	0603	1.6	0.85	0.55	70°C, 1000h: ±(0.05% R + 0.01Ω) 70°C, 8000h: ±(0.1% R + 0.02Ω)
PHP00603E2910BST1◊	291	±0.1%	0.375	0603	1.63	0.81	0.51	70°C, 2000h: ±(R + 0.1%)
PLT0603Z2910LBTS◊	291	±0.01%	0.15	0603	1.63	0.81	0.51	70°C, 2000h: ±(R + 0.1%)

♥ Vishay BC Components
♠ Vishay Foil Resistors
✦ Vishay Dale
◊ Vishay Thin Film

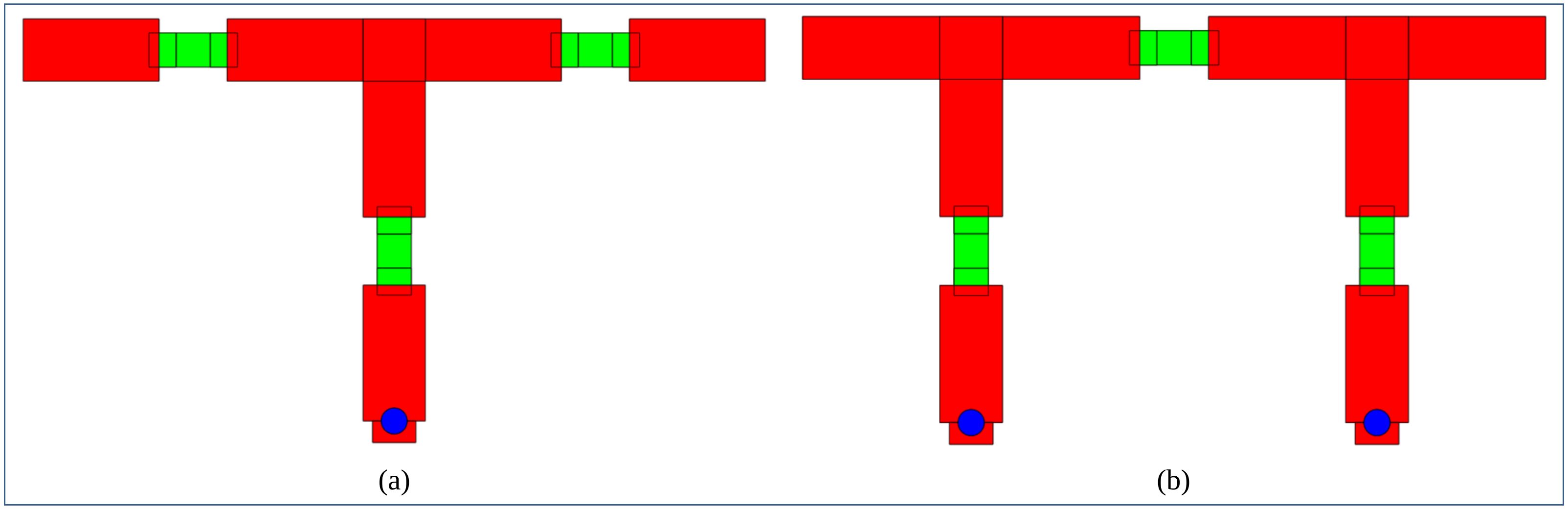

Figure 1.15 Resulting PM: (a) T and (b) Π attenuator layouts

Table 1.10 T attenuator alternative resistors

Manufacturer Part Number	**Resistance (Ω)**	**Tolerance**	**Power (W)**	**Package**	**Dimensions**			**Selected?**
					L (mm)	**W (mm)**	**H (mm)**	
ERJ3GEYJ8R2V♣	8.2	±5%	0.1	0603	1.6	0.8	0.55	
ERJ2GEJ8R2♣	8.2	±5%	0.063	0402	1.0	0.5	0.4	✓
ERJ3GEYJ121♣	120	±5%	0.1	0603	1.6	0.8	0.55	
ERJ2GEJ121♣	120	±5%	0.063	0402	1.0	0.5	0.4	✓
ERJ3GEYJ220♣	22	±5%	0.1	0603	1.6	0.8	0.55	
ERJ2GEJ220♣	22	±5%	0.063	0402	1.0	0.5	0.4	✓

♣ Panasonic Electronic Components

Table 1.11 Π attenuator alternative resistors

Manufacturer Part Number	Resistance (Ω)	Tolerance	Power (W)	Package	Dimensions			Selected?
					L (mm)	W (mm)	H (mm)	
ERJ3GEYJ180♣	18	±5%	0.1	0603	1.6	0.8	0.55	
ERJ2GEJ120♣	12	±5%	0.063	0402	1.0	0.5	0.4	✓
ERJ2GEJ5R6♣	5.6	±5%	0.063	0402	1.0	0.5	0.4	✓
ERJ3GEYJ271♣	270	±5%	0.1	0603	1.6	0.8	0.55	
ERJ2GEJ271♣	270	±5%	0.063	0402	1.0	0.5	0.4	✓
ERJ3GEYJ220♣	22	±5%	0.1	0603	1.6	0.8	0.55	
ERJ2GEJ220♣	22	±5%	0.063	0402	1.0	0.5	0.4	✓

♣ Panasonic Electronic Components

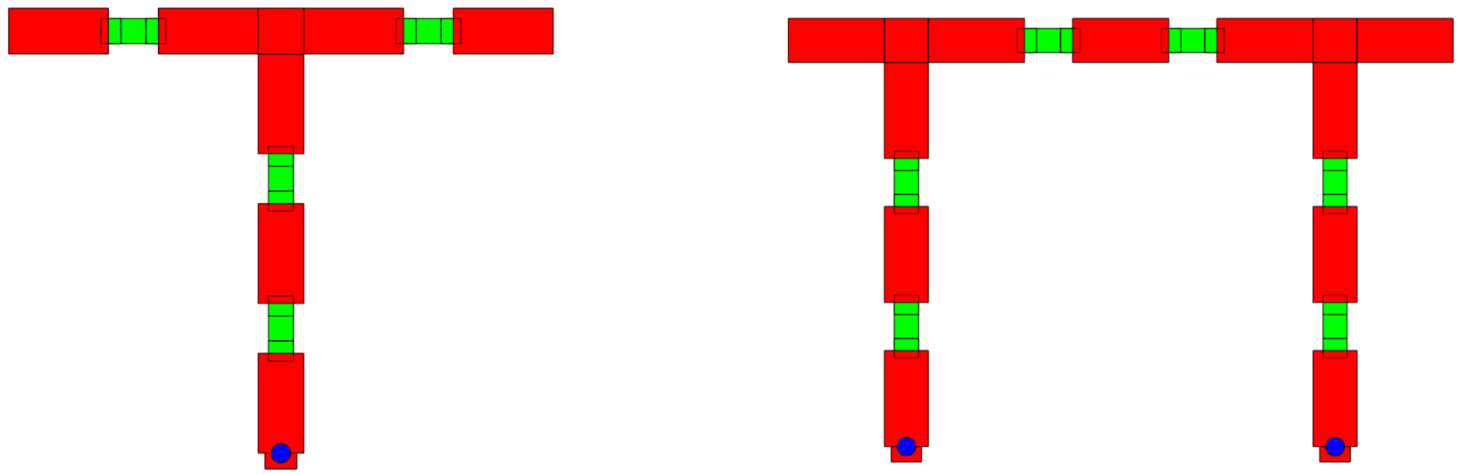

(a) (b)

Figure 1.16 Resulting PM after granularity refinement: (a) T and (b) Π attenuator layouts

Table 1.12 Form factor of initial and refined PIMs for both T and Π attenuators

	Initial PIM			**Refined PIM**		
	Length (mm)	**Width (mm)**	**Area (mm^2)**	**Length (mm)**	**Width (mm)**	**Area (mm^2)**
T attenuator	10.8966	6.223	67.80954	10.8966	9.2202	100.46883
Π attenuator	10.8204	6.223	67.33534	13.7922	9.2202	127.16684

Table 1.13 Intra-view transformation used for the attenuators' PSM granularity refinement

Consider R_{old} a vector of the old resistors to replace

Consider R_{new} a vector of the new resistors to replace the old ones with

Consider k a vector containing the number of new resistors

Step 1: Replacement of resistors

1.1. For each series resistor i in R_{old}, replace with $k(i)$ resistors in R_{new} according to the topology depicted in Figure 1.13.a

1.2. For each shunt resistor j in R_{old}, replace with $k(j)$ resistors in R_{new} according to the topology depicted in Figure 1.13.b

Step 2: Synthesis of transmission lines and circuit topology

2.1. For each transmission line:

Consider the properties given in the following:

$$\begin{cases} Z_{ci} = Z_{reference} \\ E_i = E_{default} \\ F_i = F_0 \\ A_i = A_{default} \end{cases}$$

where Z_{ci} is the characteristic impedance of the transmission line, E_i is its electrical length, F_i is the frequency at which the electrical length is calculated and A_i is the transmission line loss (in dB).

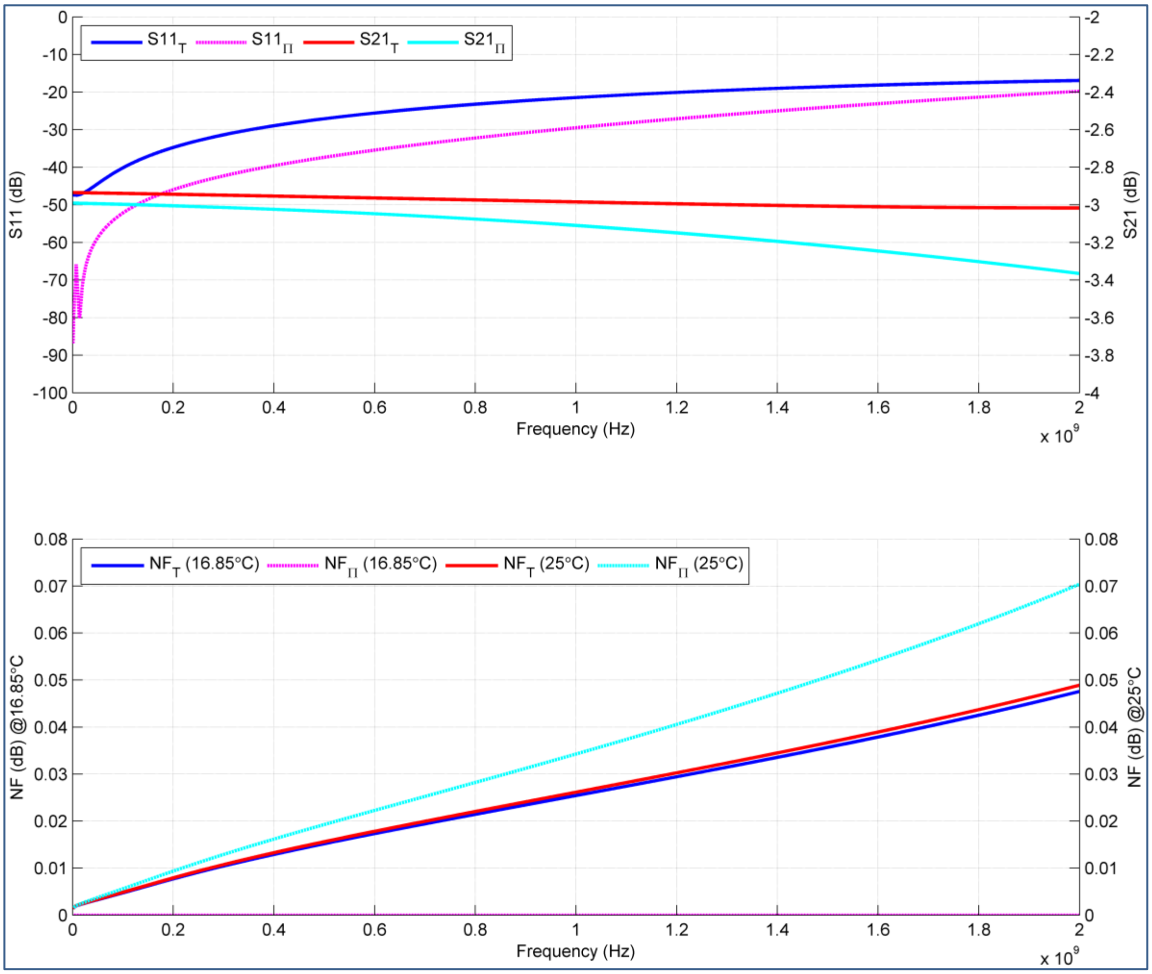

Figure 1.17 A comparison between the T and Π attenuators in terms of frequency response and noise levels (Final PM 1)

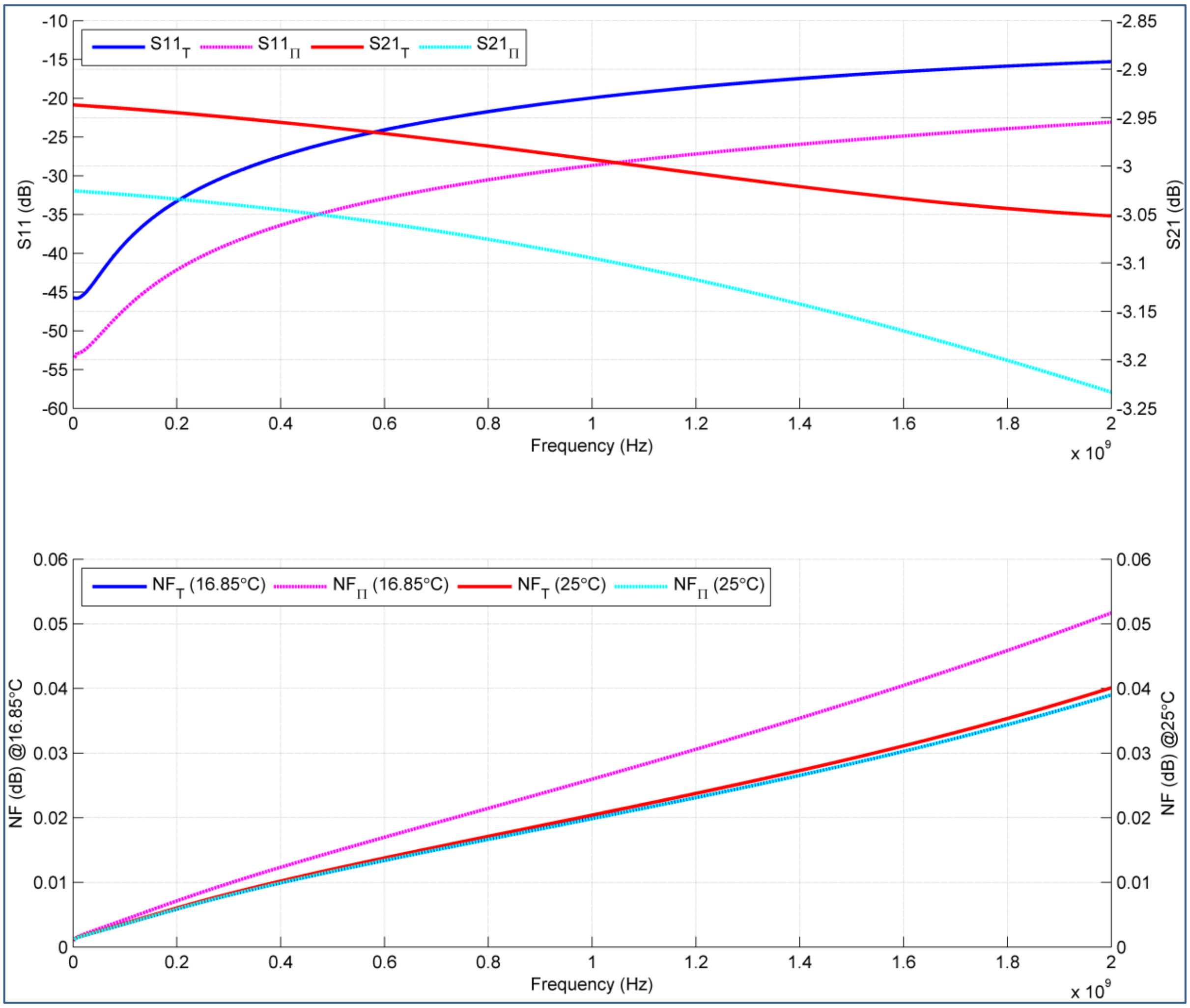

Figure 1.18 A comparison between the T and Π attenuators in terms of frequency response and noise levels (final PM after granularity refinement)

```
- <Qmatrix>
    <!-- 3-dB Resistive Attenuator -->
    <!-- Author: Sabeur LAFI -->
    <!-- version: 0.1 -->
    <Qblock name="T_att_specs" source="pim_rm_cv_01"> </Qblock>
  - <Qblock name="T_att_lumped" source="pim_rm_bbx_model_01">
    + <config></config>
    + <data></data>
    - <misc>
        <meta name="description" content="attached noise data"/>
        <dataset name="noise data" size="10" data-format="dB" temp="16.85" tempUnit="C">
        - <datapoint>
            <freq unit="Hz">1000000 </freq>
            <minNF>8.83091945e-006 </minNF>
            <GammaS data-format="MA">0.607172002 </GammaS>
            <Phase unit="deg">-179.953593 </Phase>
            <effNoiseRes unit="ohm">1.43704347e-007 </effNoiseRes>
          </datapoint>
        + <datapoint></datapoint>
        + <datapoint></datapoint>
        + <datapoint></datapoint>
        + <datapoint></datapoint>
        + <datapoint></datapoint>
        + <datapoint></datapoint>
        + <datapoint></datapoint>
        + <datapoint></datapoint>
        + <datapoint></datapoint>
        </dataset>
      + <dataset name="noise data" size="3000" data-format="dB" temp="25" tempUnit="C"></dataset>
      </misc>
    </Qblock>
    <Qblock name="T_att_LC_Mic_ideal" source="psm_trans_output_01"> </Qblock>
    <Qblock name="T_att_LC_Mic_mapping" source="psm_tech_mapping_01"> </Qblock>
    <Qblock name="T_att_LC_Mic_mapping_ref" source="psm_gran_ref_01"> </Qblock>
    <Qblock name="T_att_hybrid_sim_1" source="pm_perf_assess_01"> </Qblock>
    <Qblock name="PI_att_specs" source="pim_rm_cv_01"> </Qblock>
    <Qblock name="PI_att_lumped" source="pim_rm_bbx_model_01"> </Qblock>
    <Qblock name="PI_att_LC_Mic_ideal" source="psm_trans_output_01"> </Qblock>
    <Qblock name="PI_att_LC_Mic_mapping" source="psm_tech_mapping_01"> </Qblock>
    <Qblock name="PI_att_LC_Mic_mapping_ref" source="psm_gran_ref_01"> </Qblock>
    <Qblock name="PI_att_hybrid_sim_1" source="pm_perf_assess_01"> </Qblock>
  </Qmatrix>
```


Mandatory Qblock data sections (config, data)

Noise temperature

Additional noise data section

Figure 1.19 Noise data is supported in the Qmatrix through metadata

2 CASE STUDY II: FREQUENCY TRANSLATION DEVICE

2.1 Introduction

In the previous chapter, we studied how the proposed design framework can be applied to the design of a linear resistive component such as a RF attenuator. In this section, we use the proposed framework for the design of a nonlinear component, namely mixer.

2.2 Specifications

A radiofrequency mixer is a nonlinear frequency translation device that creates the sum and the difference from input frequencies (see Figure 2.1). A local oscillator is generally used to generate the signal frequency that mixes with the RF one.

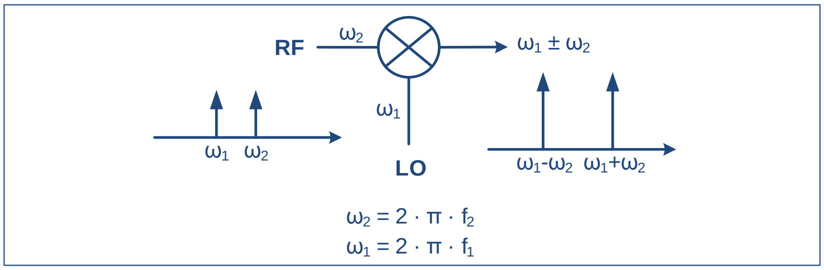

Figure 2.1 A mixer makes a frequency translation

The common specifications of RF mixers include the input frequencies, the signal power rates and the port-to-port isolations. Table 2.1 enumerates the specifications we consider for this design case study.

2.3 Functional Description: SysML requirements and platform-independent models

Similarly to the previous case studies, the first step is the mixer functional description. The package diagram of Figure 2.2 illustrates the main SysML models used to capture the mixer's specifications. The mixer structure is detailed in the « Mixer Definition » package. The mixer requirements are captured in the « Mixer Requirements » package while the coherence verification rules are comprised in the « Mixer Coherence Rules » one. All packages use the definitions given in « Value Types » one.

Table 2.1 Mixer specifications

Conversion Gain (dB)	> -9.5
RF Frequency (MHz)	2400 – 2485
LO Frequency (MHz)	2302.5
IF Frequency (MHz)	140
IF Bandwidth (MHz)	5
LO Power (dBm)	max. 8
RF Power (dBm)	-20
IF Power (dBm)	0
LO-RF Rejection (dB)	> 20 dB
LO-IF Rejection (dB)	> 30 dB
Termination Impedance (ohm)	50

- Mixer structure: a mixer is a nonlinear three port network for frequency translation. This definition is captured in the hierarchy illustrated in the bdds of Figure 2.3 and Figure 2.4. The « Three-Port Network » block is composed of three « Ports ». Its properties are inherited from the « Nonlinear Device » block. The « Frequency Translation Device » is a specialization of « Nonlinear Device » and a generalization of « Mixer Device » blocks. The specifications of Table 2.1 are captured in the properties of each block. Tables 2.2 and 2.3 show the value of each of these properties.
- Mixer requirements: the bdd of Figure 2.5 depicts a generic hierarchy of the mixer requirements. In this example, the performance requirements which include conversion gain and port-to-port isolation, are considered.
- Mixer coherence rules: the coherence verification rules that are used at the step of coherence verification are included in the « Coherence Rules » package. The Figure 2.6 depicts the PIM-level design rules.
- Value types: all the packages use the definitions included in « Value Types » package comprising for example units (see Figure 2.7).

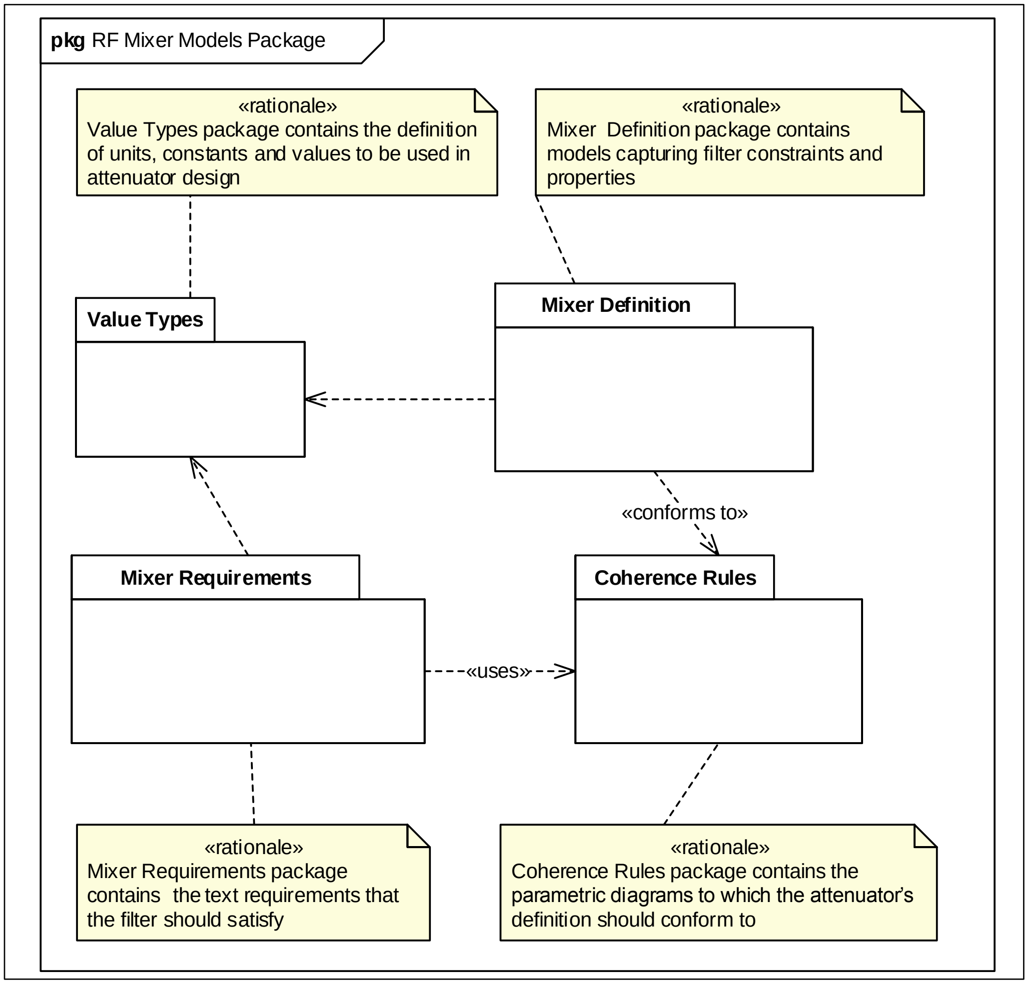

Figure 2.2 Mixer package diagram

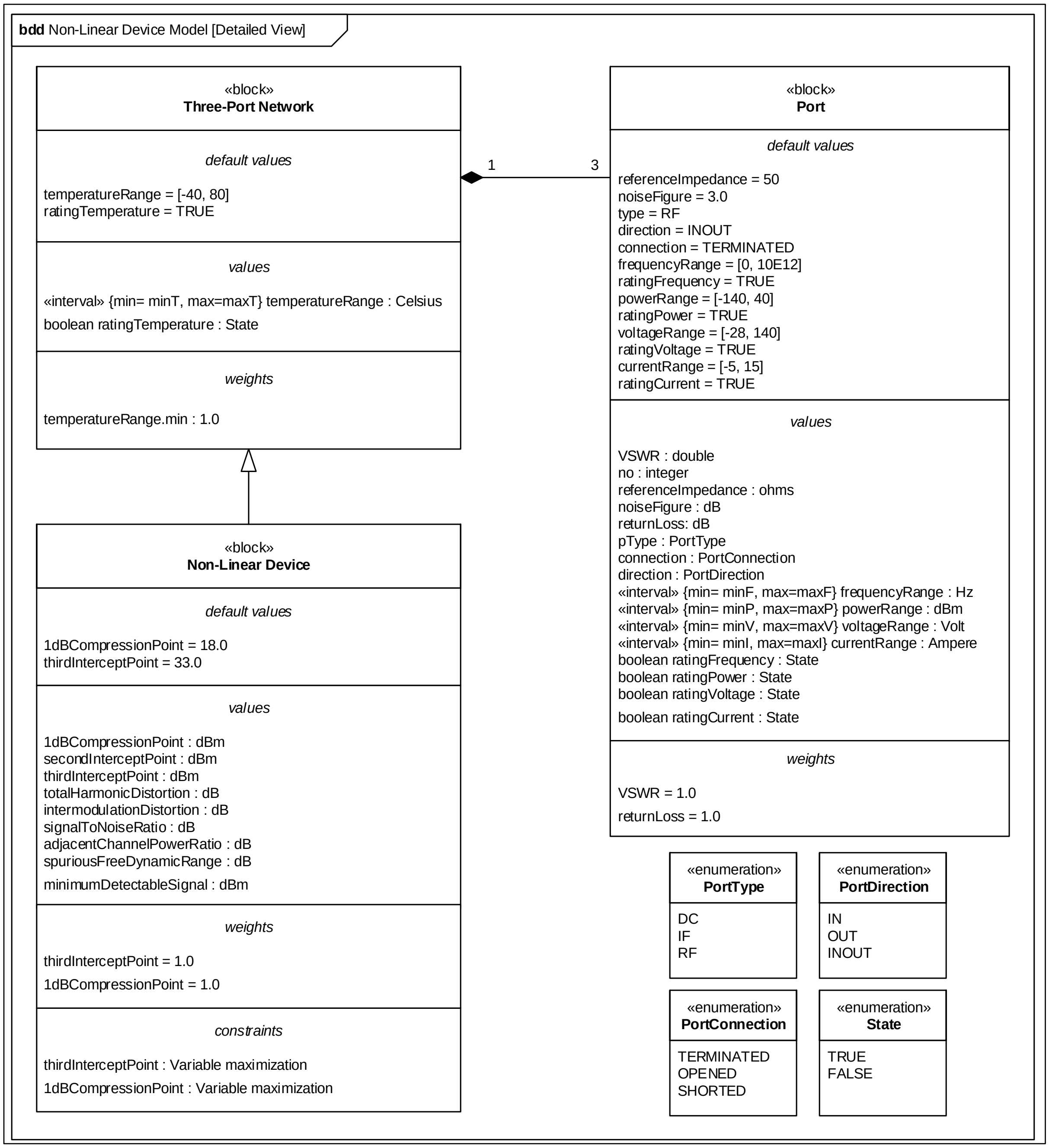

Figure 2.3 Three-port network detailed block definition diagram

2.4 Analysis: Coherence verification

The next step after functional description is the coherence verification test. The coherence rules for a nonlinear device (such as a mixer) are similar to those enumerated in the previous case studies.

Let us consider the following notations:

C_G	Conversion gain
C_{Gcomp}	Conversion gain compression
C_{Gflat}	Conversion gain flatness
F_{IF}	Frequency at IF port
F_{LO}	Frequency at LO port
F_{RF}	Frequency at RF port
P_{1dB}	1-dB compression point
P_{IF}	Power at IF port
P_{LO}	Power at LO port
$P_{LOdrive}$	LO drive level
P_{RF}	Power at RF port
R_{LOIF}	LO-IF rejection
R_{LORF}	LO-RF rejection
Z_{ref}	Reference impedance
$ACPR$	Adjacent channel power ratio
BW	Bandwidth
IMD	Intermodulation distortion
$IP2$	Second-intercept point
$IP3$	Third-intercept point
MDS	Minimum detectable signal
NF	Noise figure
RL	Return loss
$SFDR$	Spurious-free dynamic range

THD Total harmonic distortion

$VSWR$ Voltage standing wave ratio

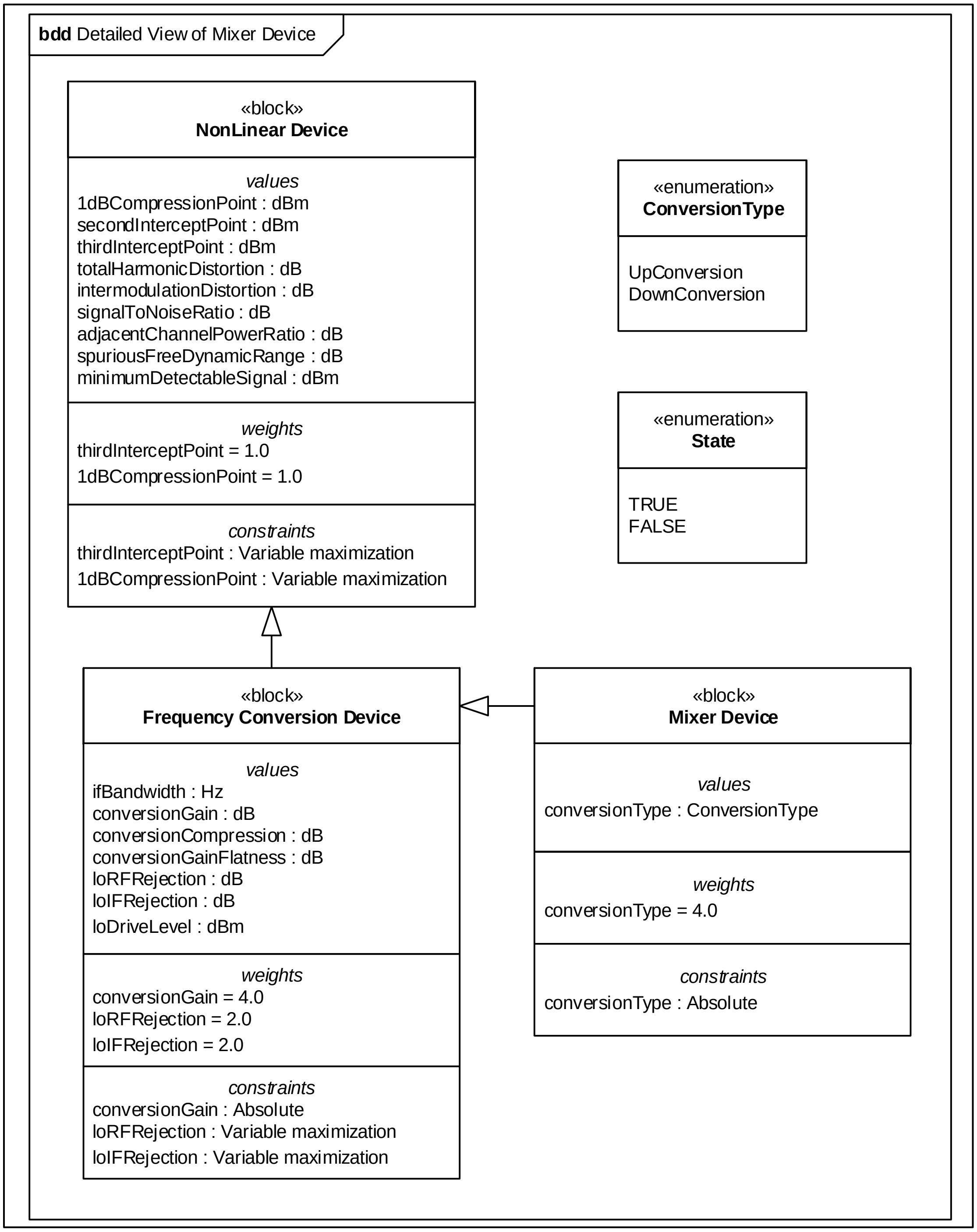

Figure 2.4 Mixer is a nonlinear frequency conversion device (Figure 2.3 cont'd)

Table 2.2 List of mixer value properties as presented in the corresponding bdds

Parameter Value	**Type**	**Default Value**	**Remarks**	**Specifications Value**
temperatureRange	interval (Celsius)	[-40, 80]		
ratingTemperature	Boolean	TRUE	TRUE FALSE	
noiseFigure	dB	3		
portList	Object (Port)			3
portsNo	integer	2		
1dBCompressionPoint	dBm	18.0		
secondInterceptPoint	dBm			
thirdInterceptPoint	dBm	33.0		
totalHarmonicDistortion	dB			
intermodulationDistortion	dB			
signalToNoiseRatio	dB			
adjacentChannelPowerRatio	dB			
spuriousFreeDynamicRange	dB			
minimumDetectableSignal	dBm			
ifBandwidth	Hz			5E6
conversionGain	dB			max. -9.5
conversionCompression	dB			
conversionGainFlatness	dB			
loRFRejection	dB			min. 20
loIFRejection	dB			min. 30
loDriveLevel	dBm			max. 8.0
conversionType	ConversionType		UPCONVERSION DOWNCONVERSION	DOWNCONVERSION

Table 2.3 List of mixer port value properties as enumerated in the SysML models

Value Property	**Type**	**Default Value**	**Remarks**	**Specifications Value**
VSWR	double			
no	integer			1 (2) (3)
referenceImpedance	double (ohms)	50.0		50 (50) (50)
returnLoss	dB			
noiseFigure	dB	3.0		
pType	PortType	RF	DC IF RF	
direction	PortDirection	INOUT	IN OUT INOUT	
connection	PortConnection	TERMINATED	TERMINATED OPENED SHORTED	
frequencyRange	interval (Hz)	[0, 10E12]		2.4425E9 (2.3025E9) (140E6)
ratingFrequency	Boolean	TRUE	TRUE FALSE	
powerRange	interval (dBm)	[-140, 40]		-20 (8.0) (0)
ratingPower	Boolean	TRUE	TRUE FALSE	
voltageRange	interval (Volts)	[-28, 140]		
ratingVoltage	Boolean	TRUE	TRUE FALSE	
currentRange	interval (Amperes)	[-5, 15]		
ratingCurrent	Boolean	TRUE	TRUE FALSE	

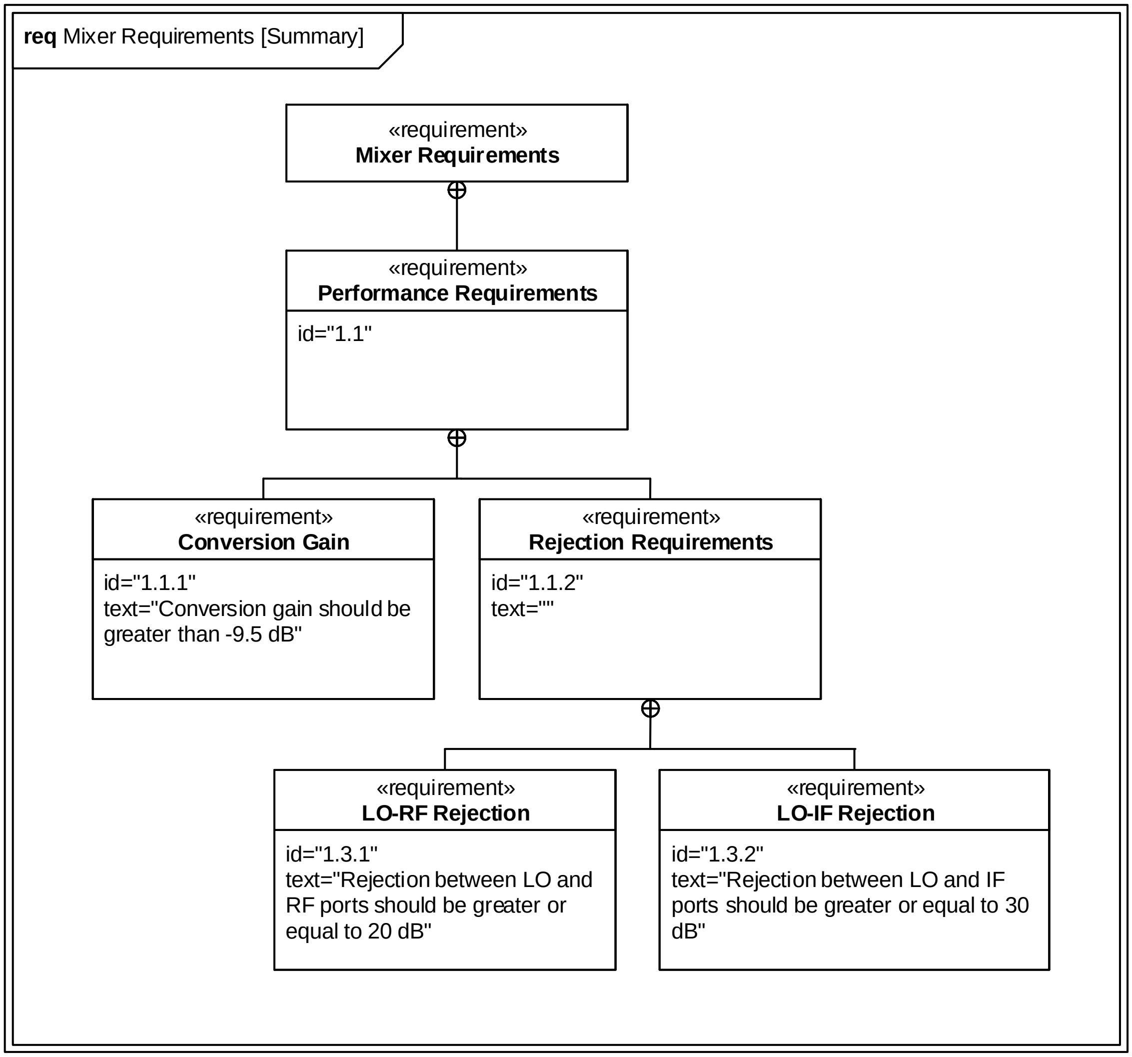

Figure 2.5 Summary of mixer requirements

The mixer coherence rules are of three types:

- PIM-level design constraints' rules: these rules ensure that the PIM-level design candidate is feasible. The rules C.1 through C.5 in Table 2.4 ensure that the mixer properties are within a feasible design extent;
- The electrical consistence rules: these rules ensure that the relationships between the mixer properties are valid. The parameters relationships graph (PRG) depicted in Figure 2.8 and the corresponding equations given in Table 2.5 allow to figure out if there are any contradictory mixer specifications;

– The integrity control rules: this type of rules ensure that the mixer properties are within a predefined acceptable range. Table 2.6 enumerates 35 rules which ensure the integrity of the mixer properties.

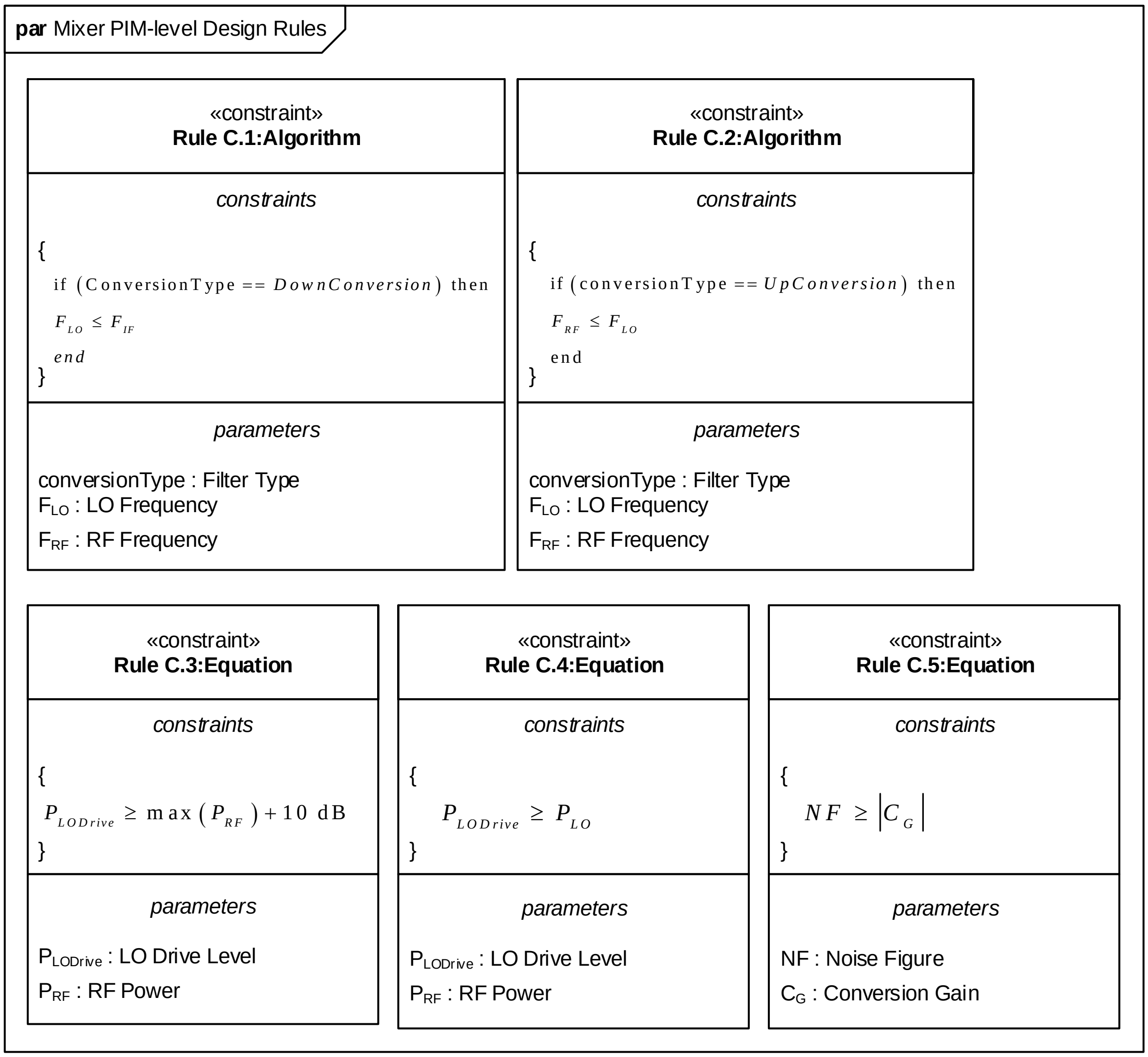

Figure 2.6 Coherence rules: PIM-level design rules

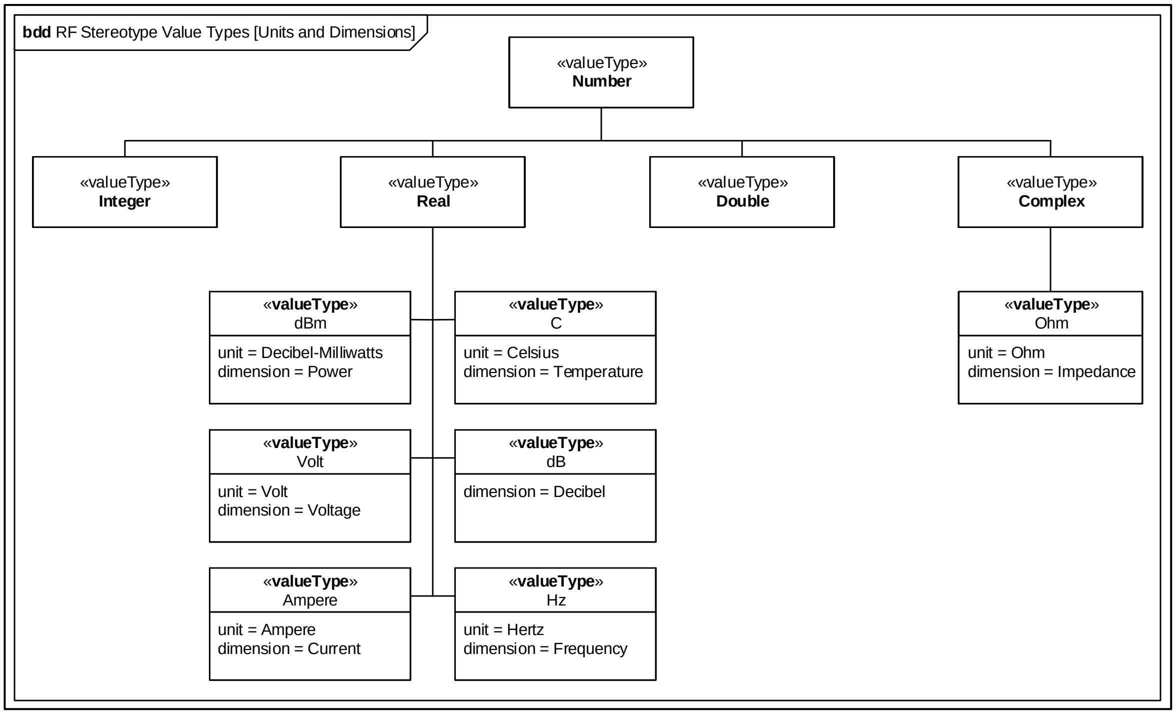

Figure 2.7 Mixer value types package

Table 2.4 Mixer PIM-level design constraints rules

No	Rule	if test fails
C.1	if $ConversionType = DownConversion$ then $F_{LO} \leq F_{RF}$ end	Error
C.2	if $ConversionType = UpConversion$ then $F_{LO} \geq F_{RF}$ end	Error
C.3	$P_{LODrive} \geq \max(P_{RF})$+10 dB	Warning
C.4	$P_{LODrive} \geq P_{LO}$	Error
C.5	$NF \geq \lvert C_g \rvert$	Warning

The mixer functional description was submitted to the coherence verification test. The results are depicted in the coherence verification report of Figure 2.9. As illustrated in this report, the rule C.5 throws a warning message. In fact, the noise figure should be greater or equal to the conversion gain. If the conversion gain was given (i.e., $C_G \leq -9.5$ dB), the noise figure was not specified in the mixer specifications. For calculations, the default property value (i.e., $NF = 3.0$ dB) was considered. However, the default value violates this rule. To keep the specifications coherent, the noise figure property is either defined by the user or overridden by the conversion gain one.

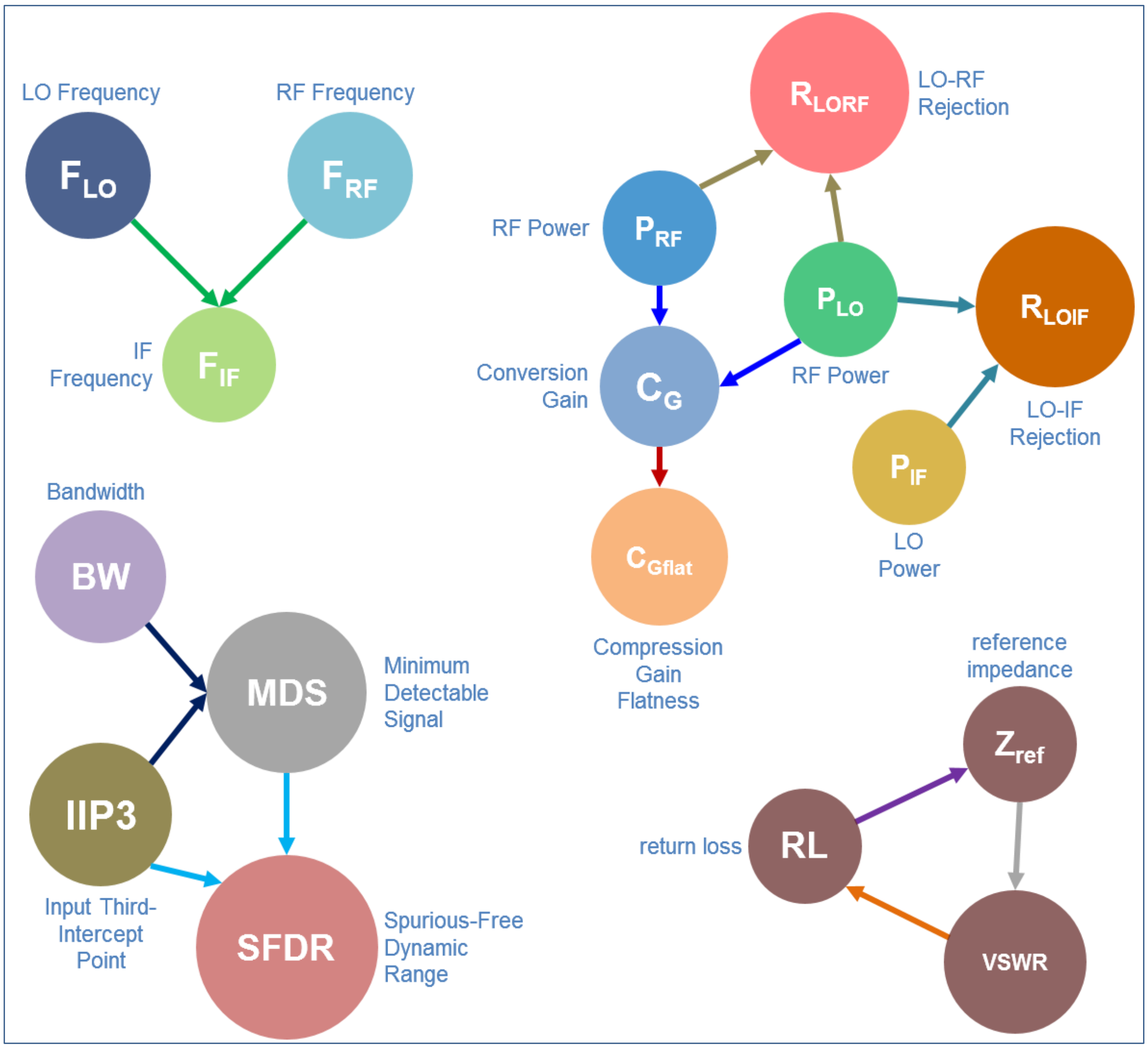

Figure 2.8 Mixer parameters relationships graph

2.5 Analysis: PIM-level granularity refinement and simulation

After coherence verification test, we proceed to the search of a PIM-level design solution. At this level, we consider as black-box model the mathematical expression for RF frequency mixing given in the equation A-4 (APPENDIX A, p. 81). The analysis of the mixer RM/PIM models using this black-box model allow a preliminary design solution. This one provides an output spectrum as illustrated in Figure 2.10.

The black-box model performance is not satisfactory. It requires more adjustments for better performance results. This can be done using a PIM-level granularity refinement process. However, we choose to skip this step in this case study.

Table 2.5 Common relationships between mixer parameters given in Figure 2.8

Arrow Color	Mathematical Relationship	Parameter
●	$C_G = P_{IF} - P_{RF}$	Compression Gain
●	$C_{Gflat} = \max(\lvert C_g \rvert) - \min(\lvert C_g \rvert)$	Compression Gain Flatness
●	$F_{IF} = F_{RF} \pm F_{LO}$	IF Frequency
●	$R_{LORF} = P_{LO} - P_{RF}$	LO-RF Rejection
●	$R_{LOIF} = P_{LO} - P_{IF}$	LO-IF Rejection
●	$MDS = \frac{2}{3}[IIP3 - 10 \cdot \log(k \cdot T \cdot BW)]$	Minimum Detectable Signal
●	$SFDR = \frac{2}{3}[IIP3 - MDS]$	Spurious-Free Dynamic Range
●	$VSWR = \frac{10^{\frac{RL}{20}} + 1}{10^{\frac{RL}{20}} - 1}$	Voltage Standing Wave Ratio
●	$RL = \frac{Z_L - Z_S}{Z_L + Z_S}$	Return Loss

Table 2.6 Mixer integrity control rules

No.	Rule	if test fails
I.1	$-80 \leq \text{temperatureRange} \leq 100$	Error or/and Warning
I.2	$\text{ratingTemperatureRange} \in \{\text{TRUE,FALSE}\}$	Error
I.3	$1 \leq \text{VSWR} \leq 10$	Error or/and Warning
I.4	$\text{no} \in \mathbb{N}^*$	Error
I.5	$0 < Z_{ref} \leq 10^4$	Error or/and Warning
I.6	$0 \leq \text{NF} \leq 10^2$	Error or/and Warning
I.7	$0 < RL \leq 120$	Error or/and Warning
I.8	$\text{ptype} \in \{\text{DC,IF,RF}\}$	Error
I.9	$\text{connection} \in \{\text{TERMINATED,OPENED,SHORTED}\}$	Error
I.10	$\text{direction} \in \{\text{IN,OUT,INOUT}\}$	Error
I.11	$0 \leq \text{frequencyRange} \leq 10^{12}$	Error or/and Warning
I.12	$0 \leq \text{powerRange} \leq 160$	Error or/and Warning
I.13	$0 \leq \text{voltageRange} \leq 10^4$	Error or/and Warning
I.14	$0 \leq \text{currentRange} \leq 10^2$	Error or/and Warning
I.15	$\text{ratingFrequency} \in \{\text{TRUE, FALSE}\}$	Error
I.16	$\text{ratingPower} \in \{\text{TRUE, FALSE}\}$	Error
I.17	$\text{ratingVoltage} \in \{\text{TRUE, FALSE}\}$	Error
I.18	$\text{ratingCurrent} \in \{\text{TRUE, FALSE}\}$	Error
I.19	$-100 \leq P_{1dB} \leq 100$	Error or/and Warning
I.20	$-100 \leq IP2 \leq 100$	Error or/and Warning
I.21	$-100 \leq IP3 \leq 100$	Error or/and Warning
I.22	$0 \leq \text{THD} \leq 120$	Error or/and Warning
I.23	$0 \leq \text{IMD} \leq 120$	Error or/and Warning
I.24	$0 \leq \text{SDR} \leq 120$	Error or/and Warning
I.25	$0 \leq \text{ACPR} \leq 120$	Error or/and Warning
I.26	$0 \leq \text{SFDR} \leq 120$	Error or/and Warning
I.27	$0 \leq \text{MDS} \leq 120$	Error or/and Warning
I.28	$0 < BW \leq 10^{12}$	Error or/and Warning

No.	Rule	if test fails
I.29	$-100 \leq C_G \leq 100$	Error or/and Warning
I.30	$-100 \leq C_{Gcomp} \leq 100$	Error or/and Warning
I.31	$0 \leq C_{Gflat} \leq 120$	Error or/and Warning
I.32	$0 \leq R_{LORF} \leq 120$	Error or/and Warning
I.33	$0 \leq R_{LOIF} \leq 120$	Error or/and Warning
I.34	$-200 \leq P_{LOdrive} \leq 120$	Error or/and Warning
I.35	conversionType ∈ {UPCONVERSION, DOWNCONVERSION}	Error

```
******** Coherence Verification Test ********
TARGET PIM: 2.4425-GHz PASSIVE MIXER (C:\Users\slafi\Documents\Design\2.4425ghz_mix.xml)

-> Electrical Consistence Rules (9 found)
    ................................................ PASS
-> PIM-level Design Constraints Rules (5 found)
     RULE C.5..................................... WARNING
          Desc.: Noise Figure property (Default Value: 3.0)
                 must be greater or equal to Abs(Conversion
                 Gain) (User-Defined: 9.5)!
-> Integrity Control Rules (35 found)
    ................................................ PASS
    Summary: (1) Warnings (0) Errors
```

Figure 2.9 Mixer coherence verification report

2.6 Analysis: PSM generation

The PIM-level solution (i.e., black-box model) is then submitted to a suitable transformation to generate one or many PSMs for each target platform. We consider in the following two PIM-to-PSM transformations which derive a couple of design solutions for traditional PCB platform (both transformations are based on the design procedures of passive diode mixers in (Sayre, 2008, pp. 383-388):

a) Passive diode mixer PIM-to-PSM transformation

This first transformation is detailed in Table 2.7. It produces a passive single-ended diode mixer in three steps:

1. **Step 1: Selection of input and output capacitors and inductors**

In the first step, we select suitable capacitors' and inductors' values for the input and output sections of a traditional single-ended diode mixer topology.

2. **Step 2: Selection of diode**

In the second step, we select a diode model (either ideal or semi-ideal) for best possible operation (e.g., power rating). It is important to notice that no technology characteristics are considered yet. The diode is considered as an electrical model that has a mathematically-computable electrical behavior.

3. **Step 3: Synthesis of circuit topology**

Finally, the transformation derives the topology of Figure 2.11.a by connecting the discrete elements and diodes as required.

b) Rat-race Mixer PIM to PSM transformation

The second transformation is detailed in Table 2.8. This transformation generates a PSM in three steps. The first one is dedicated to the selection of the suitable operation diodes. Next, an output IF filter is designed as detailed in the transformation of Table 2.10. Finally, it generates the PSM topology as illustrated in Figure 2.11.b.

Table 2.7 Passive diode mixer PIM-to-PSM transformation

Step 1: Selection of input and output capacitors and inductors 1.1. Select the values of input capacitor C_1 and inductor L_1 in a way that the ratio $r_1 = \frac{C_1}{L_1} \gg 1$ (r_1 should be as large as possible). 1.2. Select the values of input capacitor C_2 and inductor L_2 in a way that the ratio $r_2 = \frac{C_2}{L_2} \gg 1$ (r_2 should be as large as possible). **Step 2: Selection of diode** 2.1. Select a suitable operation passive diode D_1.

Step 3: Synthesis of circuit topology
3.1. Generate the circuit topology as depicted in Figure 2.11.a.

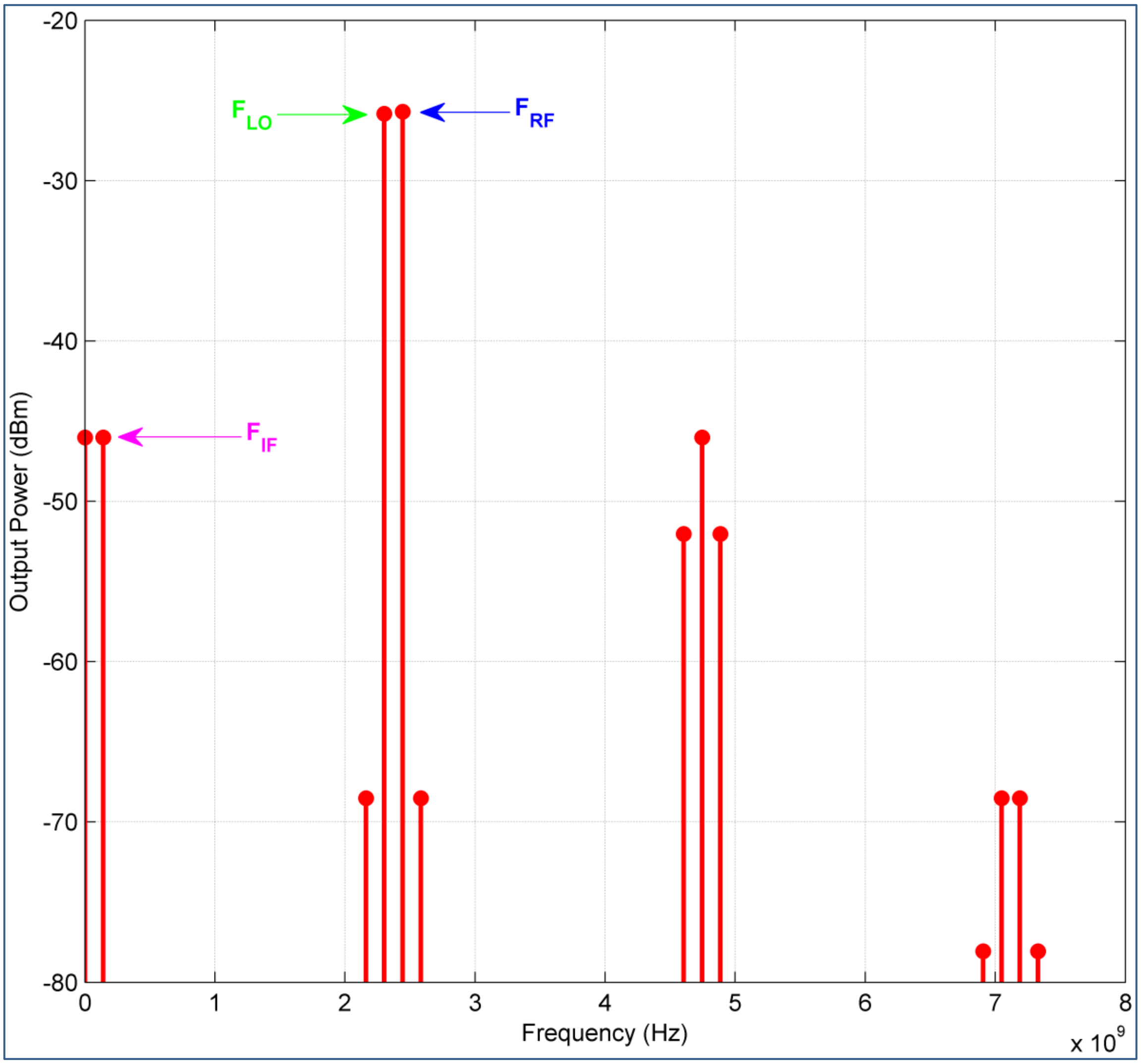

Figure 2.10 Black-box model frequency response

Table 2.8 Rat-race Mixer PIM to PSM transformation

Consider the properties for each transmission-line section:

$$\begin{cases} Z_{ci} = Z_{reference} \\ E_i = E_{default} \\ F_i = F_0 \\ A_i = A_{default} \end{cases}$$

where Z_{ci} is the characteristic impedance of the transmission line, E_i is its electrical length, F_i is the frequency at which the electrical length is calculated and A_i is the transmission line loss (in dB).

Step 1: Selection of diodes

1.1. Select suitable operation passive diodes D_1 and D_2.

Step 2: Design of output IF filter

2.1. Design an LC bandpass filter centered at F_{IF} and bandwidth BW as given in the transformation of Table 2.11 (Lafi, 2016a).

Step 3: Synthesis of transmission lines and circuit topology

3.1. Generate the circuit topology as depicted in Figure 2.11.b.

3.2. For transmission-line sections A, consider the following properties:

$$\begin{cases} Z_{ci} = 70.7\ \Omega \\ E_i = 90° \\ F_i = \dfrac{F_{RF} + F_{LO}}{2} \\ A_i = A_{default} \end{cases}$$

3.3. For transmission-line section B, consider the following properties:

$$\begin{cases} Z_{ci} = 70.7\ \Omega \\ E_i = 270° \\ F_i = \dfrac{F_{RF} + F_{LO}}{2} \\ A_i = A_{default} \end{cases}$$

On the opposite of the PIM-to-PSM transformations used in the previous case studies, the transformations applied to the mixer PIM do not directly generate the PSM artefacts from their PIM counterparts. The relationship between the PIM and the PSM entities is implicit. However, this procedure does not violate the definition of a « model-to-model transformation » because there is still a strong semantic relationship between the source and destination models. In this case, the relationship is established mathematically where the PSM is a topology whose frequency response is an approximate function which approaches the equation-based black-box model.

The use of both PIM-to-PSM transformations results in two distinct PSMs. Figure 2.12, 2.13, 2.14 and 2.15 depict a comparison of their performance.

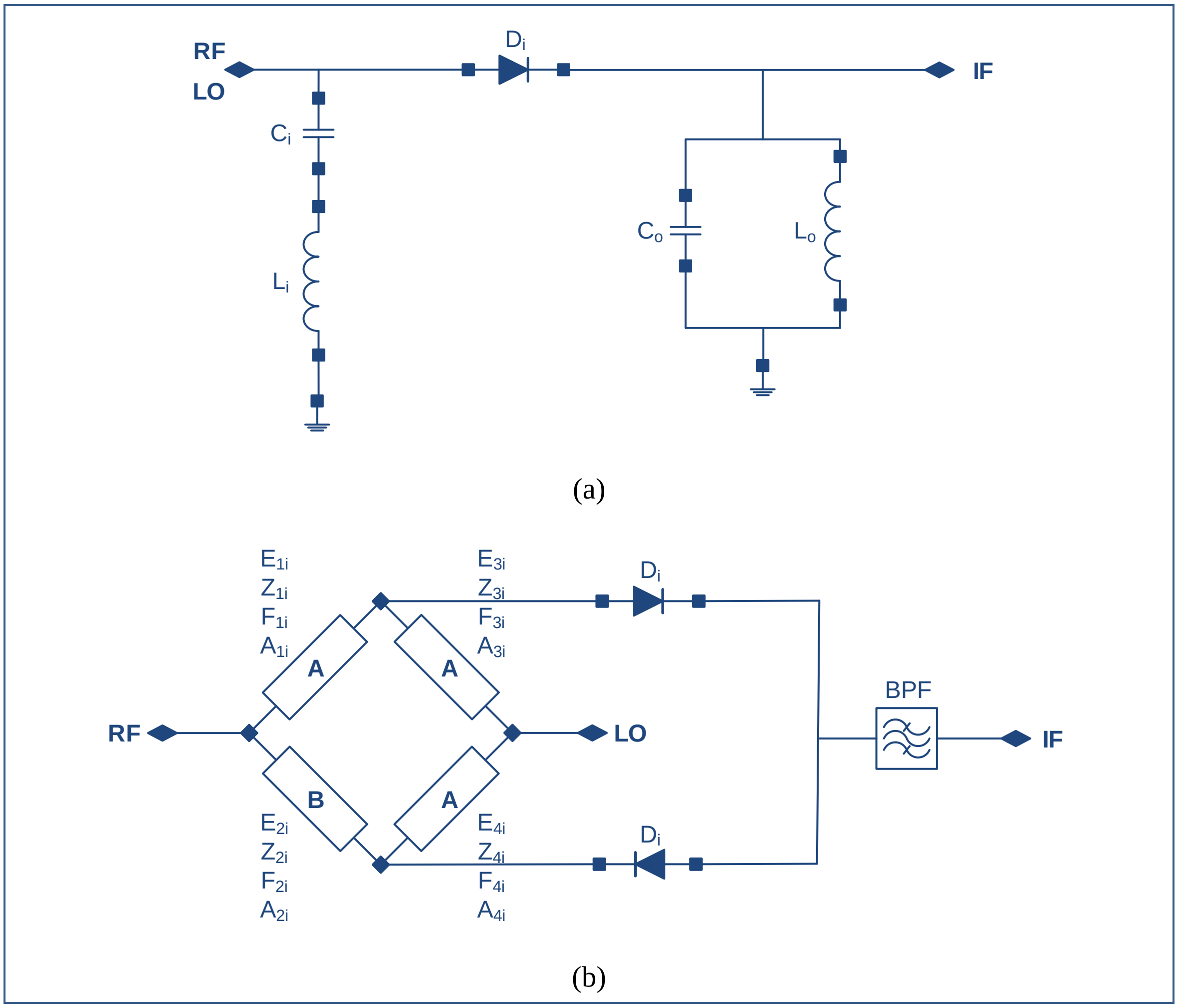

Figure 2.11 PSM topology: passive (a) single-ended diode and (b) rat-race mixer

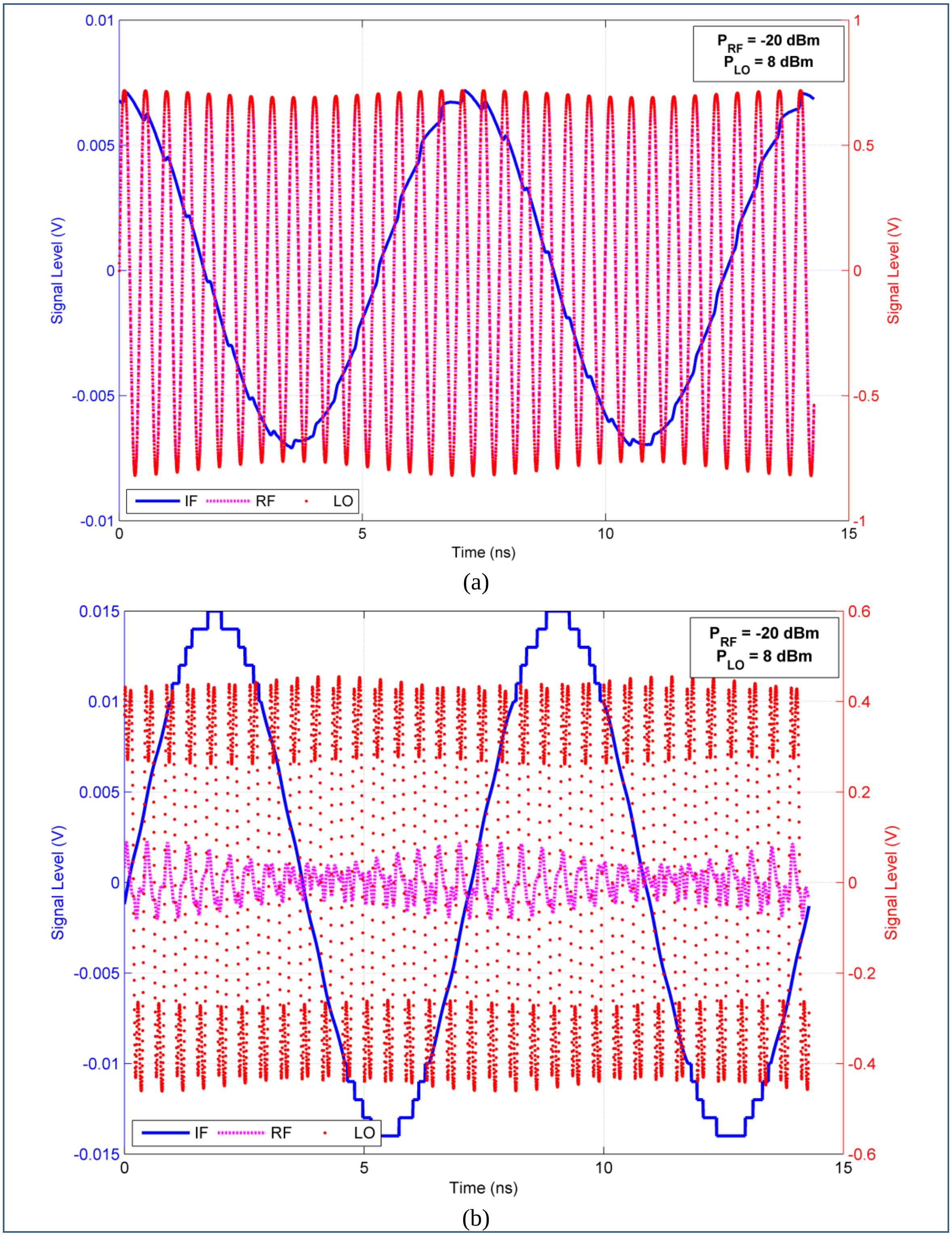

Figure 2.12 Voltage waves: (a) Single-ended and (b) rat-race diode mixer

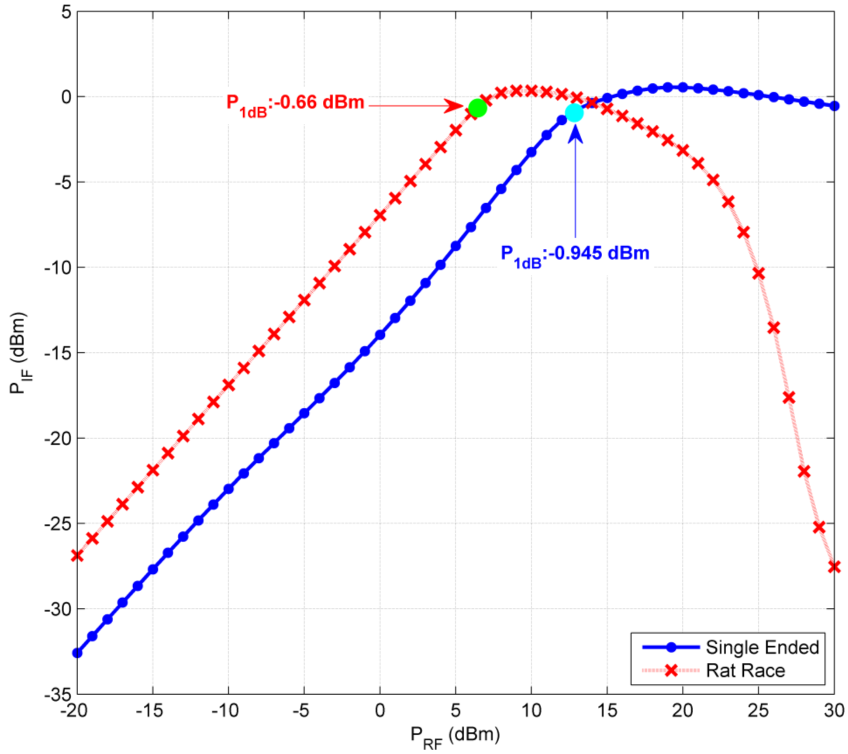

(a)

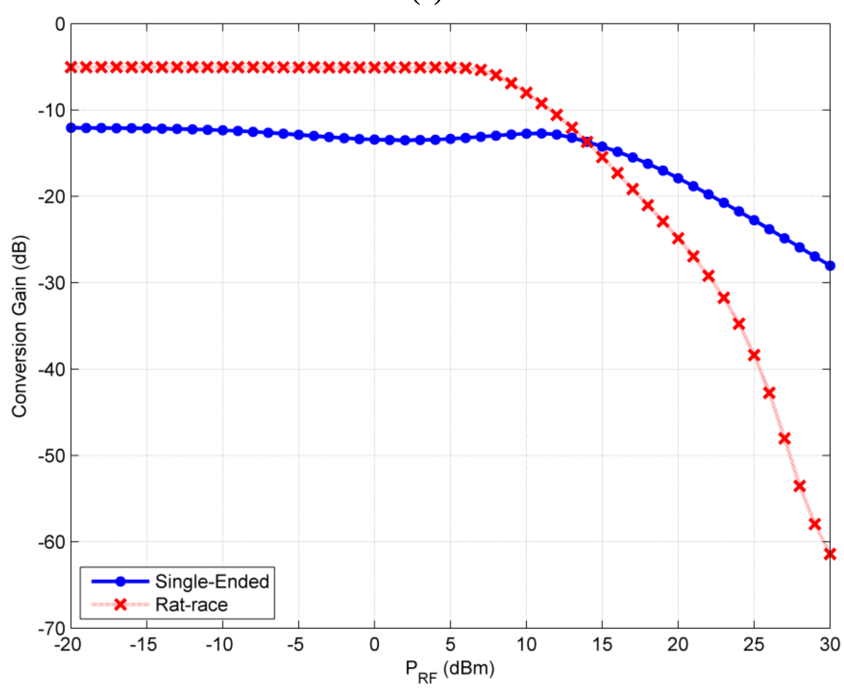

(b)

Figure 2.13 Output versus input power and (b) conversion gain of both mixers

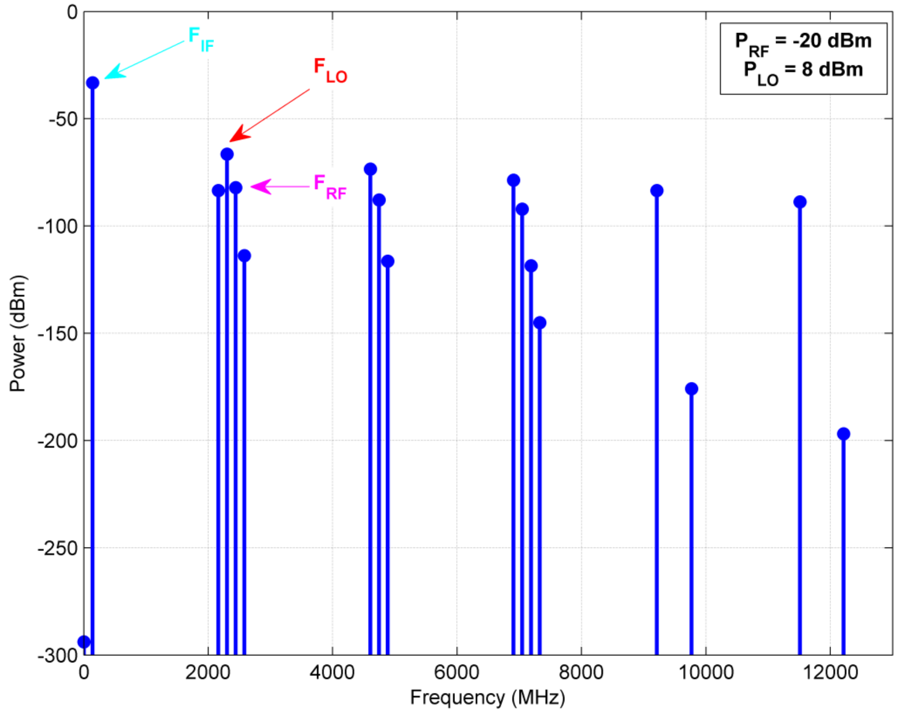

(a)

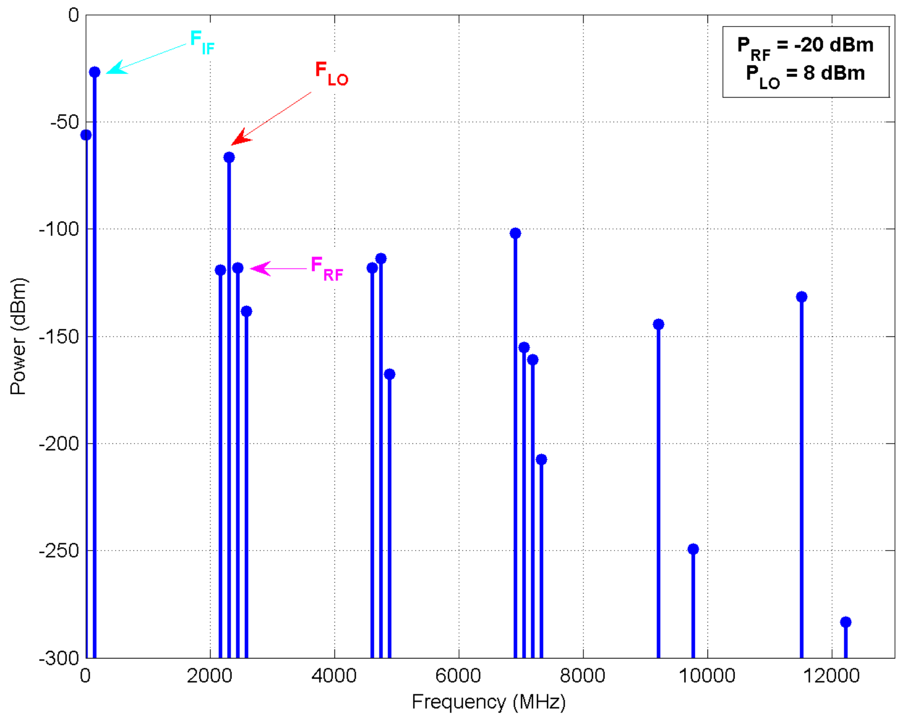

(b)

Figure 2.14 Output Spectrum: (a) Single-ended and (b) rat-race diode mixer

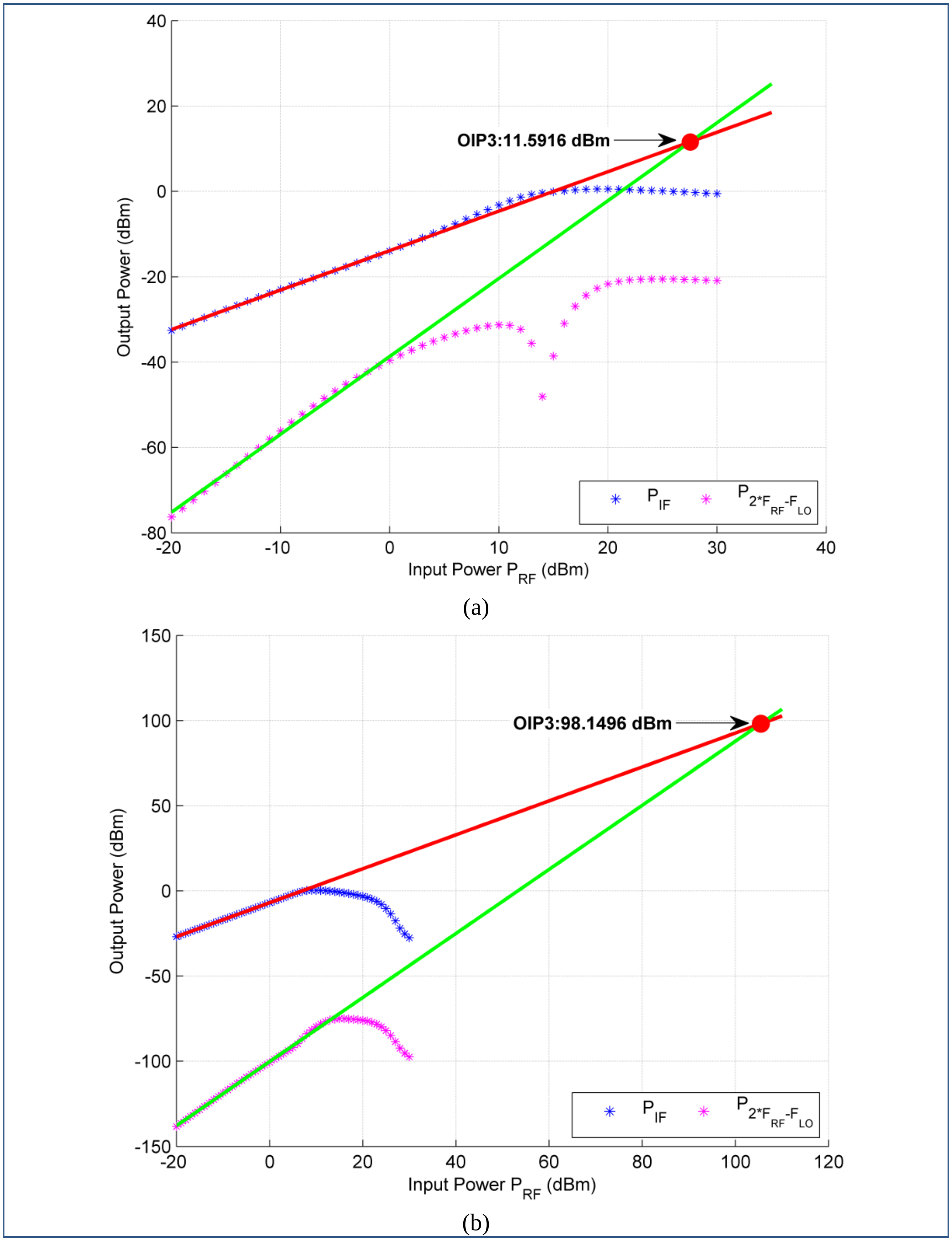

Figure 2.15 Output Third-Intercept Point: (a) Single-ended and (b) rat-race diode mixer

At this point, we need to figure out what is the best PSM in terms of performance. Table 2.9 compares the performance of each PSM against specifications. The retained metrics are conversion gain, LO-RF and LO-IF rejections as well as the 1-dB compression and the third-intercept points. The first three metrics are mandatory because they are included in the requirement diagrams. The latter ones are optional.

Table 2.9 Generated PSMs: Summary of both mixer PSMs performance characteristics

	Specifications	**Single-Ended Mixer**	**Rat-Race Mixer**
Conversion Gain (dB)	> -9.5	-12.745	-5.0965
LO-RF Rejection (dB)	> 20 dB	15.653	51.565
LO-IF Rejection (dB)	> 30 dB	33.276	39.633
1-dB Compression Point (dBm)	18[♦]	-0.945	-0.66
Third-Intercept Point (dBm)	33[♦]	11.5916	98.1496

(♦) Due to the absence of a user-defined value, default values in PSM/RM models were considered.

Table 2.10 Generated PSMs: Objective function calculations for each filter prototype

	Constant Weights C_i	**Variable Weights** X_i	
		Single-Ended Mixer	**Rat-Race Mixer**
Conversion Gain (dB)	4.0	0	1
LO-RF Rejection (dB)	2.0	$\frac{15.653}{20} = 0.78265$	$\frac{51.565}{20} = 2.57825$
LO-IF Rejection (dB)	2.0	$\frac{33.276}{30} = 1.1092$	$\frac{39.633}{30} = 1.3211$
1-dB Compression Point (dBm)	1.0	$\frac{\lvert -0.945\rvert}{18} = 0.0525$	$\frac{\lvert -0.66\rvert}{18} = 0.03667$
Third-Intercept Point (dBm)	1.0	$\frac{\lvert 11.5916\rvert}{33} = 0.3512$	$\frac{\lvert 98.1496\rvert}{33} = 2.9742$
	$\sum C_i X_i$	**2.29555**	**7.91022**

To automate the selection of the best candidate design solution, we use a decision making process that is based on an objective function. The calculations of that objective functions for both PSMs are reported in Table 2.10. The rat-race mixer PSM yields a higher score than its single-ended counterpart. This result is in accordance with the comparison performance curves already shown in Figure 2.12-2.15.

2.7 Synthesis: technology mapping

After the performance assessment of both PSMs, we retain the rat-race mixer one. We also consider at this stage that its performance is relatively satisfactory. Thus, there is no need to undertake a PSM-level granularity refinement process in the purpose of enhancing the quality of that design solution. Next, we should augment the selected PSM with the appropriate technology information. We consider the implementation of this PSM using microstrip transmission lines (see RO3006 substrate properties in Table 2.24) and lumped components. Then, the technology mapping process results in:

1- The synthesis of transmission-line sections of the rat-race mixer PSM using the substrate RO3006,
2- A search for appropriate diode parts, and
3- A search of capacitors and inductors for the output IF bandpass filter.

Using a commercial package (i.e., LineCalc), the microstrip sections are synthesized and the results are reported in Table 2.11.

We also made a search in the technology library in order to figure out the best diode parts for the selected PSM. Three candidate diodes were identified. Their properties are listed in Table 2.12.

Legend:

B_v Reverse breakdown voltage
C_{JO} Zero-bias junction capacitance
E_G Activation energy

I_{BV} Reverse breakdown current
I_S Saturation current (diode equation)
N Emission coefficient, 1 to 2
R_S Parasitic resistance (series resistance)
P_B Contact potential at periphery junction
P_T Junction periphery
M Junction grading coefficient

Table 2.11 Properties of the synthesized rat-race microstrip sections (RO3006 substrate)

Transmission Line	**Properties**					
	Width (mil)	**Length (mil)**	**Radius (mil) (Angle (°))**	**Effective Dielectric Constant**	**Total Structure Attenuation (dB)**	**Skin Depth**
Section A	17.423425	-	586.69462 (60°)	4.097	0.064	0.063
Section B	17.423425	-	586.69462 (60°)	4.097	0.064	0.063
Section C	17.423425	-	586.69462 (60°)	4.097	0.064	0.063
Section D	17.423425	-	586.69462 (180°)	4.097	0.192	0.063
Port sections	35.984449	66.122441	-	4.367	0.005	0.063

Table 2.12 List of suitable diode parts found in the technology library

Diode Parameter	**Unit**	**Manufacturer Part Name**		
		HSCH-5310♦	**HMPS-2820♦**	**HSMP-5332♦**
B_v	V	5	15	5
C_{JO}	pF	0.09	0.7	0.13
E_G	eV	0.69	0.6	0.69
I_{BV}	A	10^{-5}	10^{-4}	10^{-5}
I_S	A	$3 \cdot 10^{-10}$	$2.2 \cdot 10^{-8}$	$4 \cdot 10^{-8}$
N		1.08	1.08	1.08

R_S	Ω	13	8	9
P_B	V	0.65	0.65	0.5
P_T		2	2	2
M		0.5	0.5	0.5
Frequency range		1 GHz – 26 GHz	10 MHz – 6 GHz	1 GHz – 26 GHz
Description		Low to medium barrier beam lead Schottky diode	Low barrier beam lead Schottky diode	Medium barrier beam lead Schottky diode

♦ Avago Technologies

For IF bandpass filter inductors and capacitors, we made an automated search in the same custom technology library that we used in the previous case studies (see Figure 2.16). We found out several parts whose properties are respectively reported in Table 2.13 and 2.14.

Since we obtained three candidate diode parts with different operation properties, we derived three prototypes from the selected PSM. After the simulation of each prototype, we compared their performance using the same metrics of Table 2.9. The results are listed in Table 2.15. Then, we calculated the objective function for each prototype. As illustrated in Table 2.16, the gap between the prototypes is relatively narrow. As expected, the prototype using the low to medium barrier beam lead Schottky diode, namely HSCH-5310, performs better than the others. This observation is confirmed by its flat conversion gain for an input RF power level up to 5 dBm, as shown in Figure 2.17. On the contrary, the other diode parts show less flat conversion gain when $P_{RF} \geq 0$ dBm. This indicates that the HSCH-5310 rat-race mixer prototype is more linear and provides a safe margin for high input power levels.

```
Searching in available capacitors libraries...

Ceramic Capacitors Library (910 elements):
    Lower Edge (C)  <=  C_ideal (C) <=  Upper Edge (C)
    1.900000e-011   <=  1.936000e-011   <=  2.000000e-011       => Best value:  1.900000e-011

Aluminium Capacitors Library (399 elements):
    Lower Edge (C)  <=  C_ideal (C) <=  Upper Edge (C)
    NaN <=  1.936000e-011   <=  NaN     => Best value:  NaN

Film Capacitors Library (309 elements):
    Lower Edge (C)  <=  C_ideal (C) <=  Upper Edge (C)
    NaN <=  1.936000e-011   <=  NaN     => Best value:  NaN

Tantalum Capacitors Library (309 elements):
    Lower Edge (C)  <=  C_ideal (C) <=  Upper Edge (C)
    NaN <=  1.936000e-011   <=  NaN     => Best value:  NaN

Polymer Capacitors Library (910 elements):
    Lower Edge (C)  <=  C_ideal (C) <=  Upper Edge (C)
    NaN <=  1.936000e-011   <=  NaN     => Best value:  NaN

-------------------------------------------------------------------------------------------------------------------------------------
|  No. |  Ideal Cap. (F)  |  Ceramic Lib.   |  Aluminium  |  Film   |  Tantalum   |  Polymer |  Selected Cap. (Lib.)   |
-------------------------------------------------------------------------------------------------------------------------------------
|  C1  |  1.936000e-011   |  1.900000e-011  |  NaN        |  NaN    |  NaN        |  NaN     |  1.900000e-011 (Ceramic) |
-------------------------------------------------------------------------------------------------------------------------------------
NaN: no coherent value found
```

(a)

```
Searching in available inductors libraries...

Fixed Inductors Library:
    Lower Edge (H)  <=  L_ideal (H) <=  Upper Edge (H)
    6.200000e-008   <=  6.270100e-008   <=  6.400000e-008       => Best value:  6.200000e-008

Common-Mode-Choke Inductors Library:
    Lower Edge (H)  <=  L_ideal (H) <=  Upper Edge (H)
    NaN <=  6.270100e-008   <=  NaN     => Best value:  NaN

Adjustable Inductors Library:
    Lower Edge (H)  <=  L_ideal (H) <=  Upper Edge (H)
    5.900000e-008   <=  6.270100e-008   <=  7.000000e-008       => Best value:  5.900000e-008

-------------------------------------------------------------------------------------------------------------------------
|  No. |  Ideal Ind. (H)  |  Fixed Library  |  CMC Library |  Adjustable Library  |  Selected Value (Lib.)  |
-------------------------------------------------------------------------------------------------------------------------
|  L1  |  6.270100e-008   |  6.200000e-008  |  NaN         |  5.900000e-008       |  6.200000e-008 (Fixed)  |
-------------------------------------------------------------------------------------------------------------------------
NaN: no coherent value found
```

(b)

Figure 2.16 Technology mapping results for (a) capacitor and (b) inductor elements

Table 2.13 List of inductor parts found in the technology library during automated technology mapping

Ideal Value (nH)	Real Value (nH)	Manufacturer Part Number	Tolerance	Max. DC Resistance (Ω)	Frequency Self-Resonance (GHz)	Q @ 200 MHz	Package	Dimensions (mm)		
								L	W	H
62.701	62	LQW15AN62NG00D♣	±2%	1.82	2.6	20	0402	1	0.5	0.6
62.701	62	LQW18AN62NG00D♣	±2%	0.51	2.3	38	0603	1.6	0.8	1
62.701	62	MLG0603S62NJT000♦	±5%	1.4	1.1	5	0603	0.6	0.3	0.33
62.701	62	LQW15AN62NJ00D♦	±5%	1.82	2.6	20	0402	1	0.5	0.6

♣ Murata Electronics North America
♦ TDK Corporation

Table 2.14 List of capacitor parts found in the technology library during automated technology mapping

Ideal Value (pF)	Real Value (pF)	Manufacturer Part Number	Family	Tolerance	Dimensions (mm)		
					L	W	H
19.36	19	AQ137M190FA1BE♠	Ceramic	±1%	0.11	0.11	0.102
19.36	18	0402ZK180GBSTR♠	Thin Film	±2%	1	0.55	0.5
19.36	18	0402ZK180FBSTR♠	Thin Film	±1%	1	0.55	0.5
19.36	20	08055J200FBTTR♠	Thin Film	±1%	2.01	1.27	1.13
19.36	20	12101K220JBTTR♠	Thin Film	±5%	3.02	2.5	1.13

♠ AVX Corporation

Table 2.15 Comparison of the performance of the three PSM prototypes

	Specifications	HSCH-5310	HMPS-2820	HSCH-5332
Conversion Gain (dB)	> -9.5	-7.4281	-9.1535	-7.6307
LO-RF Rejection (dB)	> 20 dB	53.239	42.093	55.382
LO-IF Rejection (dB)	> 30 dB	36.359	33.182	33.525
1-dB Compression Point (dBm)	18[♦]	-2.511	-4.24	-4.08
Third-Intercept Point (dBm)	33[♦]	89.141237	80.415848	83.358509

(♦) Due to the absence of a user-defined value, default values in PSM/RM models were considered.

2.8 Synthesis: PM generation

We selected the technology-mapped PSM using the HSCH-5310 diode part of platform-model generation. Using a commercial design package (i.e., ADS), we generated the PM as shown in Figure 2.18.

Table 2.16 Technology mapped PSM: Objective function calculations for each rat-race mixer prototype

	Constant Weights C_i	Variable Weights X_i		
		HSCH-5310	**HMPS-2820**	**HSCH-5332**
Conversion Gain (dB)	4.0	1	1	1
LO-RF Rejection (dB)	2.0	$\frac{53.239}{20} = 2.66195$	$\frac{42.093}{20} = 2.10465$	$\frac{55.382}{20} = 2.7691$
LO-IF Rejection (dB)	2.0	$\frac{36.359}{30} = 1.212$	$\frac{33.182}{30} = 1.106$	$\frac{33.525}{30} = 1.1175$
1-dB Compression Point (dBm)	1.0	$\frac{\|-2.511\|}{18} = 0.1395$	$\frac{\|-4.24\|}{18} = 0.2355$	$\frac{\|-4.08\|}{18} = 0.02267$
Third-Intercept Point (dBm)	1.0	$\frac{\|89.141237\|}{33} = 2.7012$	$\frac{\|80.415848\|}{33} = 2.4368$	$\frac{\|83.358509\|}{33} = 2.526$
	$\sum C_i X_i$	**7.71465**	**6.88295**	**7.43527**

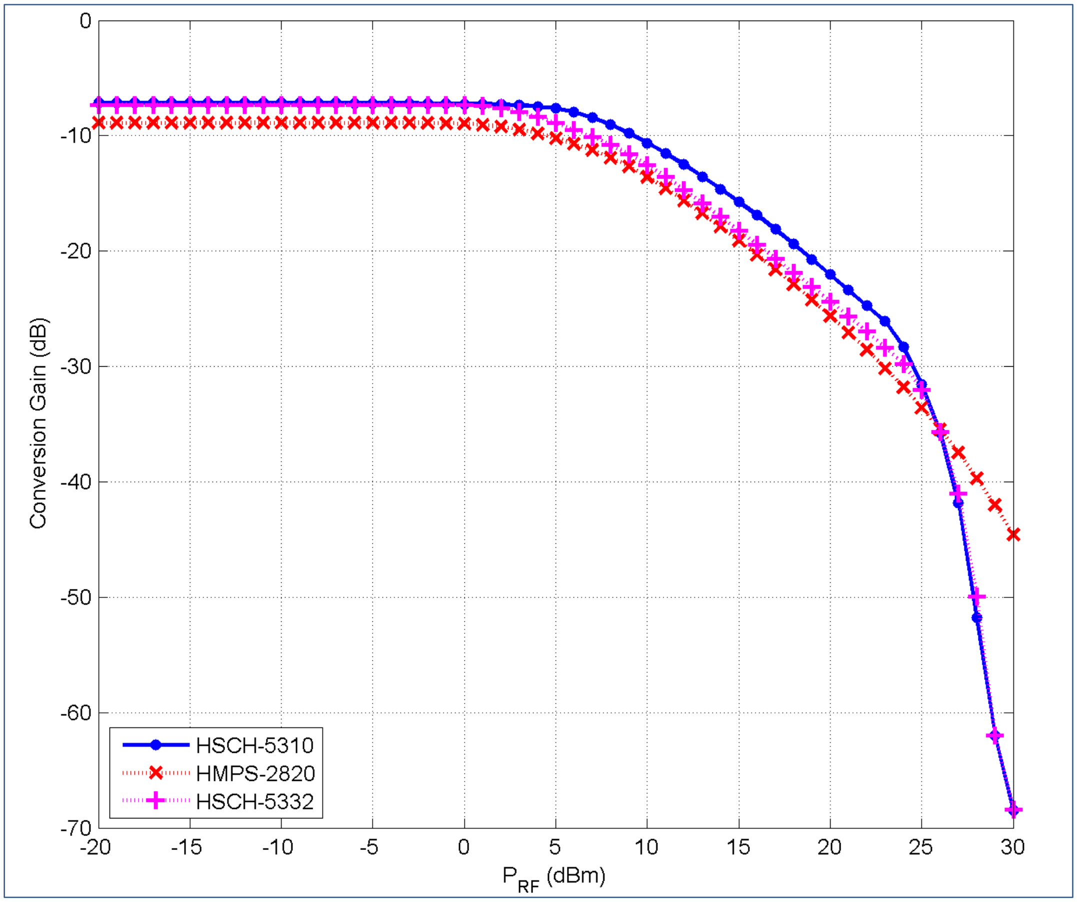

Figure 2.17 Conversion gain of the generated PSMs after technology mapping

We demonstrated in the previous case studies how the Q-matrix can be used for the design of linear circuits. The Q-matrix can be also useful for the design of nonlinear circuits such as mixers. As multidimensional structure, the Q-matrix enables, for example:

1. The storage of both linear and nonlinear data from different sources

As illustrated in Figure 2.19, it is possible to populate the Q-matrix with linear data (e.g., scattering parameters) and nonlinear data (resulting for example from harmonic balance simulations). For instance, Figure 2.19 shows a sample of scattering parameters (i.e., S_{12} and S_{21}) calculated at the frequency point 2442.5 MHz. At the same frequency, the output spectrum is computed at different frequencies including the IF located at 140 MHz.

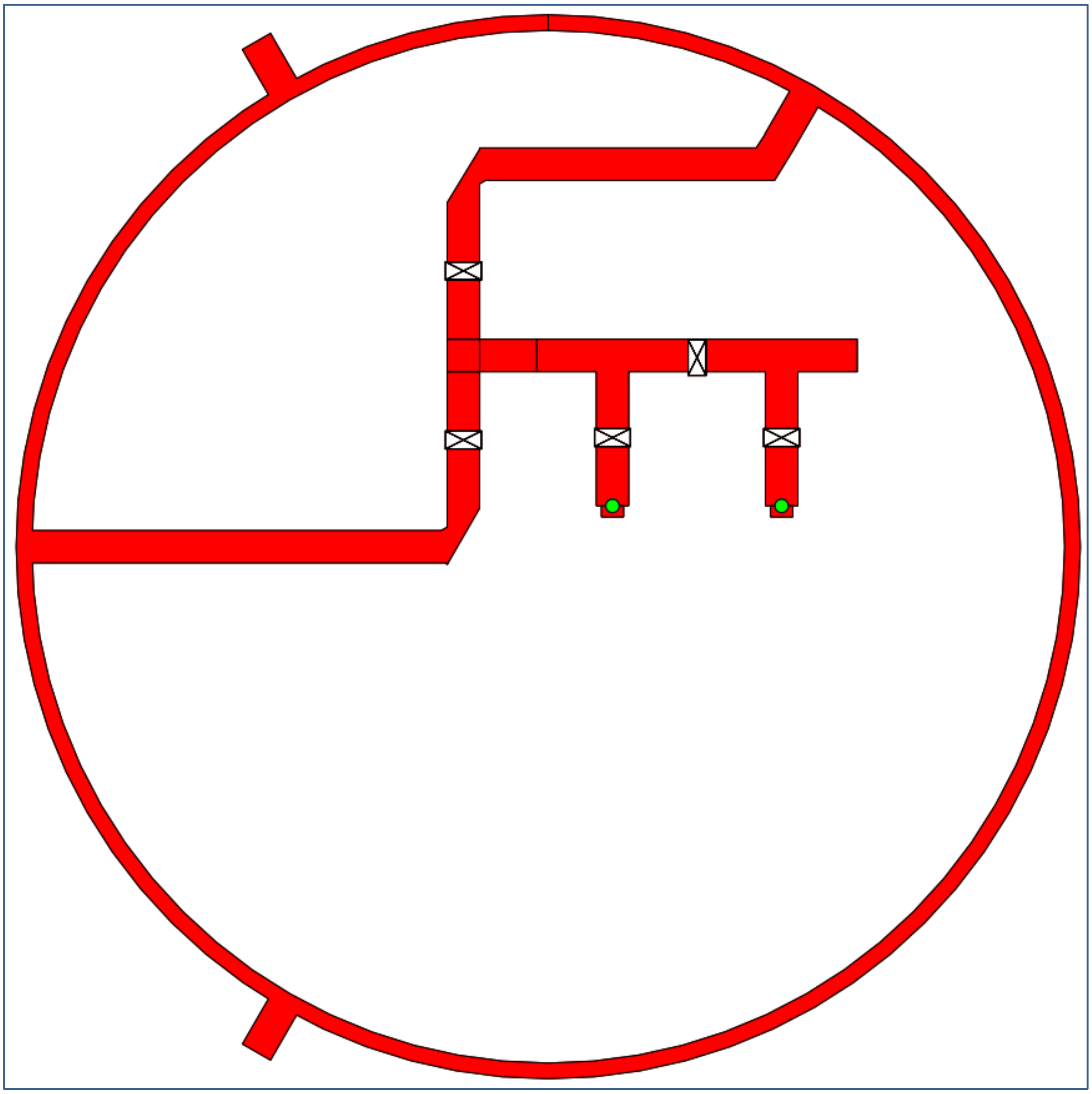

Figure 2.18 Platform Model: Layout of the final rat-race mixer

2. The use of stored data for the interpretation of various parameters without additional overhead

The « *attachedPortConfig* » XML structure stores the frequency and power levels for each port. This information can be used to calculate some properties of the circuit. For instance, it is possible to calculate the mixer's conversion gain and the output spectrum as illustrated in Figure 2.19. The conversion gain is computed using the values of the power level at input and output ports respectively. The single data point of Figure 2.19 allows to draw two spectrum rays at the input and output frequencies since the power levels are known.

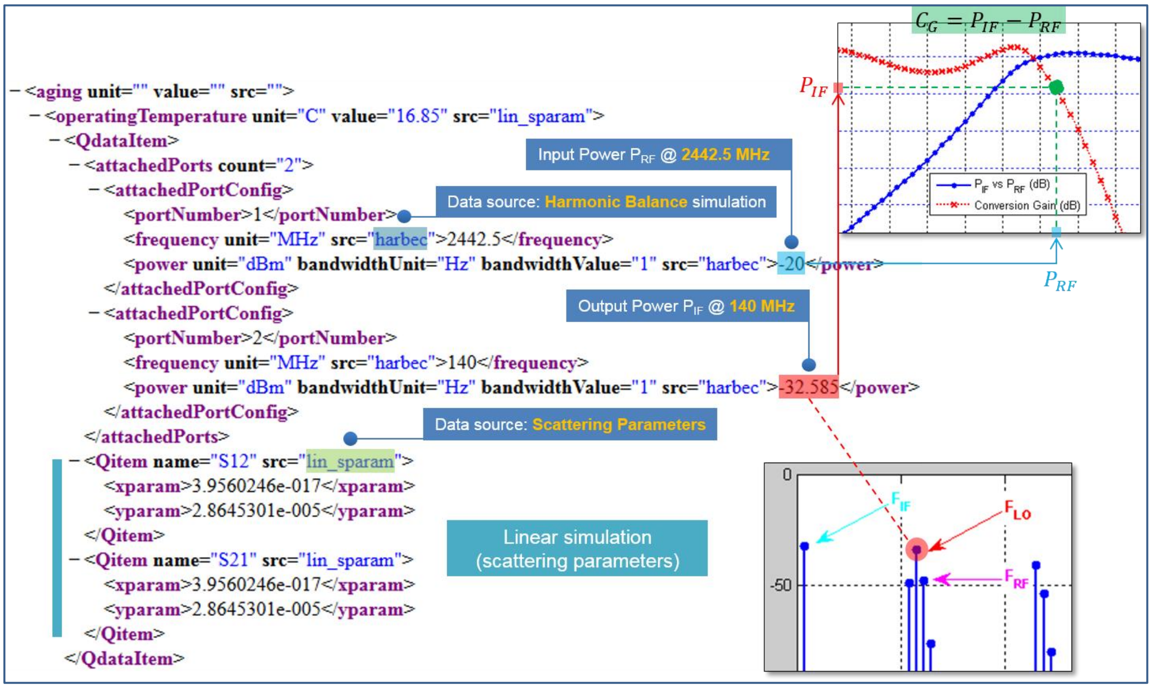

Figure 2.19 The Q-matrix stores both linear and nonlinear data

It is also possible to compute other parameters by cascading the information stored in different data points. For example, the LO-RF rejection R_{LO-RF} can be computed using the information given in two QdataItems where the output ports frequencies are respectively F_{LO} and F_{RF} (see Figure 2.20). The computation of parameters such as the output 1-dB compression and third-intercept points require relatively more complex computations of several cascaded data points (i.e., *QdataItem*).

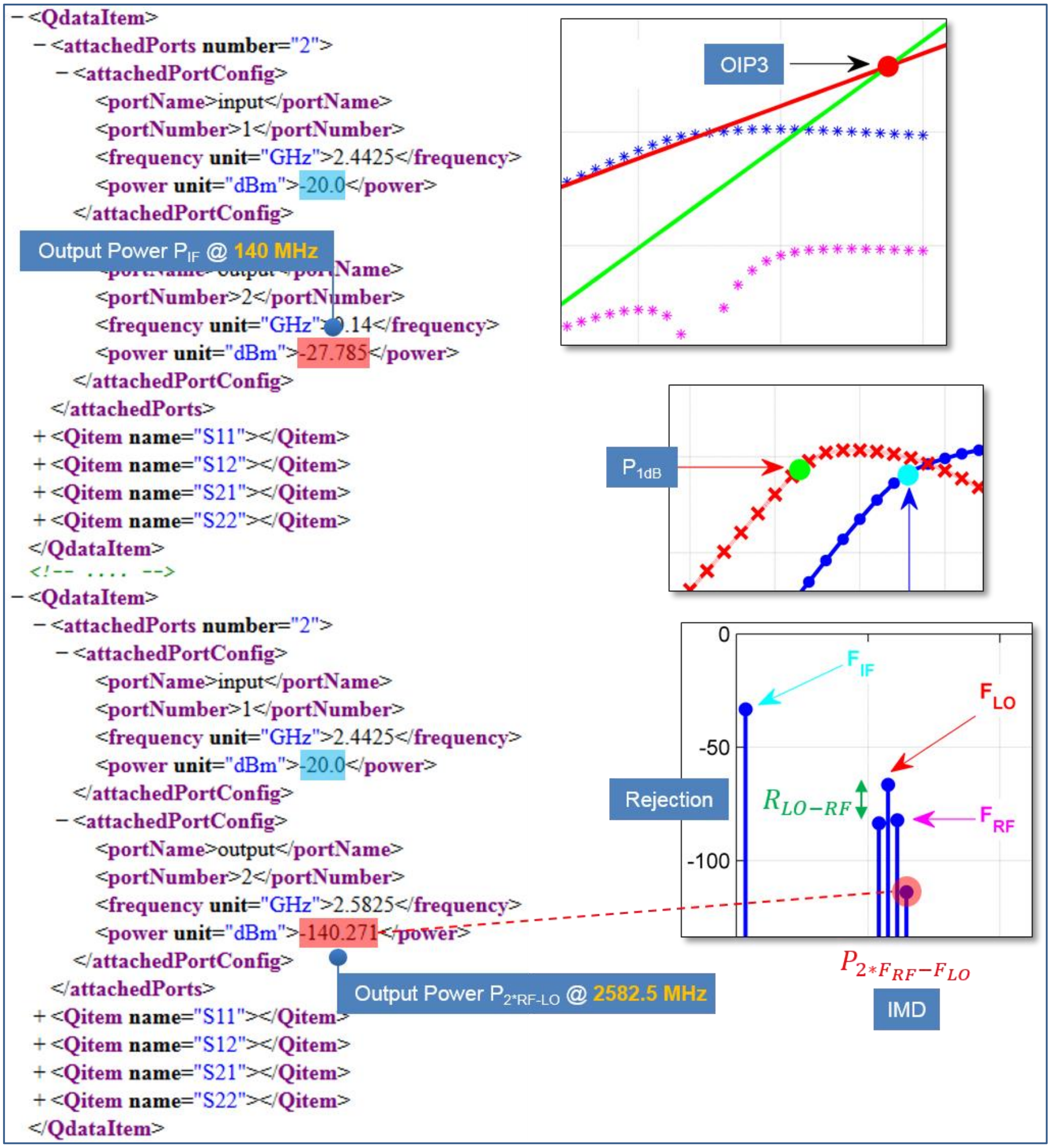

Figure 2.20 The Q-matrix stores data that can be interpreted in different ways

REFERENCES

Lafi, Sabeur, Ammar Kouki, and Jean Belzile. 2016a. *Implementation Details of a Hardware Abstraction-Based Design Methodology for Radiofrequency Circuits: Examples of Linear Devices*. Coll. "Rapport technique de l'ÉTS", ETS-RT-2016-002. Montreal, QC: École de technologie supérieure, 123 p.

Lafi, Sabeur, Ammar Kouki, and Jean Belzile. 2016b. *SysML Profile for RF Devices*, Technical report, École de technologie supérieure.

Lafi, Sabeur, Ammar Kouki, and Jean Belzile. 2015. "Enhancing Automation in RF Design Using Hardware Abstraction". In *Computational Intelligence in Analog and Mixed-Signal (AMS) and Radio-Frequency (RF) Circuit Design*, Mourad Fakhfakh, Esteban Tlelo-Cuautle, and Patrick Siarry (eds), pp. 439-469. Cham: Springer International Publishing.

Sayre, Cotter W. 2008. *Complete Wireless Design*, 2nd ed. New York: McGraw-Hill, 693 p.

APPENDIXES

APPENDIX A

SUMMARY OF EQUATIONS AND FORMULAS USED IN CASE STUDIES

B.1 Case Study 1: Radiofrequency Attenuator

B.1.1 General Definitions

- General fixed resistive attenuator transfer function:

$$H(s)|_{s=\sigma+j\omega} = \frac{V_{out}(s)}{V_{in}(s)} = K \quad \text{(A-1)}$$

where K is an attenuation factor.

B.1.2 Examples of Resistive Attenuator Pads

B.1.2.1 T-Pad Symmetric Attenuator

- Calculation of T-pad attenuator elements:

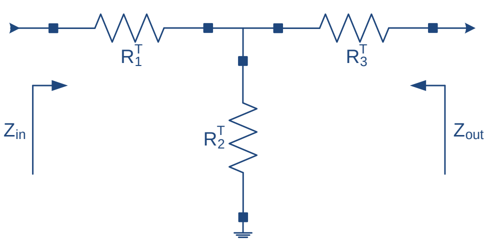

$$\begin{cases} A = 10^{Attenuation/10} \\ R_2^T = \dfrac{2\sqrt{Z_{in} \cdot Z_{out} \cdot A}}{A-1} \\ R_1^T = \left(\dfrac{A+1}{A-1}\right) Z_{in} - R_2^T \\ R_3^T = \left(\dfrac{A+1}{A-1}\right) Z_{out} - R_2^T \end{cases} \quad \text{(A-2)}$$

where Z_{in}, Z_{out} are respectively the input and output reference impedances and $Attenuation$ is the required attenuation expressed in dB.

B.1.2.2 Π-Pad Symmetric Attenuator

- Calculation of Π-pad attenuator elements:

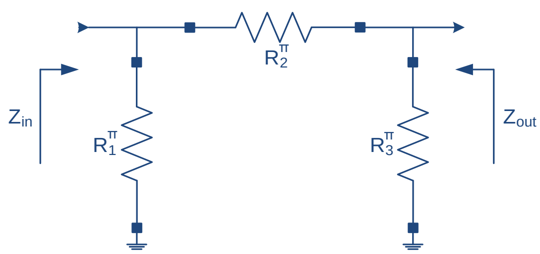

$$\begin{cases} A = 10^{Attenuation/_{10}} \\ R_2^{\pi} = \dfrac{1}{2}(A-1)\sqrt{\dfrac{Z_{in} \cdot Z_{out}}{A}} \\ R_1^{\pi} = \dfrac{1}{\dfrac{A+1}{Z_{in}(A-1)} - \dfrac{1}{R_2^{\pi}}} \\ R_3^{\pi} = \dfrac{1}{\dfrac{A+1}{Z_{out}(A-1)} - \dfrac{1}{R_2^{\pi}}} \end{cases} \quad \text{(A-3)}$$

where Z_{in} and Z_{out} are respectively the input and output reference impedances and $Attenuation$ is the required attenuation expressed in dB.

Table A.1 Main properties of the RO3006 substrate

Dielectric Constant (ε_r)	6.15
Magnetic Constant (μ_r)	1
Loss Tangent ($\tan\delta$)	0.0025
Resistivity (σ_1)	1
Metal Thickness (t)	0.71 mil
Metal Roughness (Sr)	0.075 mil
Substrate Height (h)	25 mil

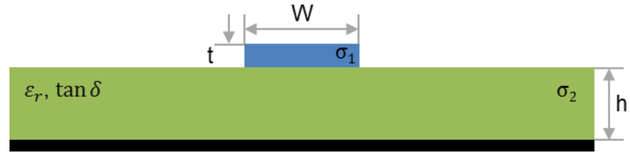

B.2 Case Study 2: RF Mixer

- General radiofrequency mixer output function:

$$V_{out} = V_{LO}V_{RF} = \frac{A_1 A_2}{2} \cdot [\cos\big((\omega_1 + \omega_2)t\big) + \cos((\omega_1 - \omega_2)t)] \quad \text{(A-4)}$$

where ω_1 (respectively ω_2) is the local oscillator (respectively RF signal) angular frequency.